How will the key marine calcifier *Emiliania huxleyi* respond to a warmer and more thermally variable ocean?

Xinwei Wang[1], Feixue Fu[2], Pingping Qu[2], Joshua D. Kling [2], Haibo Jiang[3], Yahui Gao[1,4*], David A. Hutchins[2*]

1. School of Life Sciences and State Key Laboratory of Marine Environmental Science, Xiamen University, Xiamen, 361102, China

2. Department of Biological Sciences, University of Southern California, Los Angeles, California, 90089, USA

3. School of Life Sciences, Central China Normal University, Wuhan, Hubei, China.

4. Key Laboratory of the Ministry of Education for Coastal and Wetland Ecosystems, Xiamen University, Xiamen 361102, China

*Corresponding authors: David Hutchins, tel: 1-213-7405616, fax: 1-213-7408123, Email address: dahutch@usc.edu; Yahui Gao, tel/fax: 86-592-2181386, Email address: gaoyh@xmu.edu.cn

Key words: thermal variation, *Emiliania huxleyi*, coccolithophore, calcification, growth rate, elemental composition, global warming

Abstract

Global warming will be combined with predicted increases in thermal variability in the future surface ocean, but how temperature dynamics will affect phytoplankton biology and biogeochemistry is largely unknown. Here, we examine the responses of the globally important marine coccolithophore *Emiliania huxleyi* to thermal variations at two frequencies (one-day and two-day) at low (18.5 ^{o}C) and high (25.5 ^{o}C) mean temperatures. Elevated temperature and thermal variation decreased growth, calcification and physiological rates, both individually and interactively. One-day thermal variation frequencies were less inhibitory than two-day variations under high temperature, indicating that high frequency thermal fluctuations may reduce heat-induced mortality and mitigate some impacts of extreme high temperature events. Cellular elemental composition and calcification was significantly affected by both thermal variation treatments relative to each other, and to the constant temperature controls. The negative effects of thermal variation on *E. huxleyi* growth rate and physiology are especially pronounced at high temperatures. These responses of the key marine calcifier *E. huxleyi* to warmer, more variable temperature regimes have potentially large implications for ocean productivity and marine biogeochemical cycles under a future changing climate.

Introduction

Climate-driven changes such as ocean warming alter the productivity and composition of marine phytoplankton communities, thereby influencing global biogeochemical cycles (Boyd et al., 2018; Hutchins & Fu, 2017; Thomas, et al., 2012). Increasing sea surface temperatures have been linked to global declines in phytoplankton concentration (Boyce et al., 2010), changes in spring bloom timing (Friedland et al., 2018), and biogeographic shifts in harmful algal blooms (Fu et al. 2012; Gobler et al., 2017). Warming and acidification may drive shifts away from dinoflagellate or diatom dominance, and towards nanophytoplankton (Hare et al., 2007; Keys et al., 2018). Similarly, Morán et al. (2010) predicted that a gradual shift will occur towards smaller primary producers in a warmer ocean.

Effects of temperature increases on phytoplankton diversity are uncertain. Warming and phytoplankton biodiversity were found to be inversely correlated in a coastal California diatom assemblage, at least on short timescales (Tatters et al., 2018). In contrast, a five-year long mesocosm experiment found that elevated temperature can modulate species coexistence, thus increasing phytoplankton species richness and productivity (Yvon-Durocher et al. 2015). Globally, rising temperatures may result in losses of phytoplankton biodiversity in the tropics, but gains in the polar regions (Thomas et al., 2012). It is thought that ocean warming will lead to a poleward range expansion of warm-water species at the expense of cold-water species (Boyd et al., 2010; Gao et al., 2018; Hallegraeff, 2010; Hutchins & Fu, 2017; Thomas et al., 2012). It is evident that rising ocean temperatures will benefit some groups, while having

detrimental consequences for others (Boyd et al., 2010, 2015, 2018; Feng, et al., 2017; Fu et al., 2014). For example, recent decades of satellite observations show a striking poleward shift in the distribution of blooms of the coccolithophore *Emiliania huxleyi*, a species that was previously virtually absent in polar waters (Boyd et al., 2010; Neukermans et al., 2018).

Coccolithophores are the most successful calcifying phytoplankton in the ocean, and contribute almost half of global marine calcium carbonate production. They play crucial biogeochemical roles by performing both photosynthesis and calcification, and facilitate carbon export to the deep ocean through the ballasting effects of their calcium carbonate shells (Klaas & Archer, 2002; Krumhardt et al., 2017; Monteiro et al., 2016). *E. huxleyi* (Lohm.) is the most abundant and cosmopolitan coccolithophore, forming prolific blooms in many regions (Holligan, et al., 1983; 1993; Iglesias-Rodríguez et al., 2002; Westbroek et al., 1993).

The responses of *E. huxleyi* to global change factors have been intensively investigated. Many *E. huxleyi* strains are sensitive to ocean acidification, which negatively affects their growth rates and calcification (Feng et al., 2018; Hoppe et al., 2011). However, among the many currently changing environmental drivers, temperature may be among the most important in regulating coccolithophore physiology (Boyd et al., 2010). Feng et al. (2008) reported that the growth rate of *E. huxleyi* was improved by elevated temperature at low irradiance. Furthermore, temperature was the most important driver controlling both cellular particulate organic and inorganic carbon content of a Southern Hemisphere *E. huxleyi* strain (Feng et al.,

84 2018).

85 Most research about the effects of global warming on *E. huxleyi* and
86 phytoplankton in general has focused on predicted increases in mean temperatures.
87 However, in the natural environment, seawater temperatures fluctuate over timescales
88 ranging from hours, to days, to months (Bozinovic et al., 2011; Jiang et al., 2017).
89 Future climate models predict not only in an increase in mean temperature, but also an
90 increase in temperature variability (frequency and intensity), as well as a higher
91 probability of extreme events (IPCC 2013).

92 The impacts of climatic variability and extremes have been best studied in
93 metazoans, where they may sometimes have a larger effect than increases in climatic
94 averages alone (Vázquez et al., 2017; Vasseur et al., 2014; Zander et al., 2017).
95 Variability can promote greater zooplankton species richness, compared with long-term
96 average conditions (Cáceres 1997; Shurin et al. 2010). In corals, temperature variability
97 could buffer warming stress, elevate thermal tolerance and reduce the risk of bleaching
98 (Oliver & Palumbi, 2011; Safaie et al., 2018).

99 In comparison, we still lack a thorough understanding of how thermal variation
100 affects phytoplankton growth and physiology. Unlike zooplankton, the few available
101 studies suggest increasing thermal variation may decrease phytoplankton biomass and
102 biodiversity, and shift the community towards small phytoplankton (Burgmer &
103 Hillebrand, 2011; Rasconi et al., 2017). Two studies have shown that plastic responses
104 play a key role in acclimation and adaptation to thermal fluctuations in algae (Kremer
105 et al., 2018; Schaum & Collins, 2014). Population growth rates of phytoplankton in

fluctuating thermal environments have been quantitatively modeled based on data from thermal response curves obtained under constant temperatures (Bernhardt et al., 2018).

In view of this relative lack of information on the effects of non-steady state temperatures on biogeochemically important phytoplankton, we carried out a thermal variability study using the Sargasso Sea *E. huxleyi* isolate CCMP371. Our experiments combined ocean warming with thermal variations, with a focus on the increasing frequency of temperature variations under global climate change. We examined growth rates, photosynthesis, calcification and elemental composition under constant, one-day and two-day temperature variations. This study is intended to provide insights into how different frequencies of thermal variation may influence the physiology and biogeochemistry of this important marine calcifying phytoplankton species under both current and future sea surface temperatures.

Materials and methods

The marine coccolithophore *E. huxleyi* (Lohm.) Hay and Mohler stain CCMP371 (isolated from the Sargasso Sea) was maintained in the laboratory as stock batch cultures in Aquil medium (100 μmol L^{-1} NO_3^- , 10 μmol L^{-1} PO_4^{3-}) made with 0.2 μM-filtered coastal seawater collected from the California region (Sunda et al., 2005). Cells were grown at 22 ºC under 120 μmol photons m^{-2} s^{-1} cool white fluorescent light with a 12 h/12 h light/dark cycle.

Experimental set-up

An aluminum thermal gradient block with a range of 13 temperatures was used to perform the thermal response curve and temperature variation experiments. For the

thermal curve experiment, the extreme temperatures of the thermal-block were set to 8.5 °C and 28.6 °C, with intermediate temperatures of 10.5 °C, 12 °C, 13.5 °C, 15.5 °C, 17.5 °C, 18.5 °C, 21.3 °C, 22.6 °C, 24.5 °C, 26.6 °C, and 27.6 °C. The *E. huxleyi* cells were transferred from the stock cultures into triplicate 120 ml acid washed polycarbonate bottles in the thermal block under a 12 h light /12h dark cycle at 180 µmol photons m^{-2} s^{-1}. For the light intensity measurement, irradiance was measured individually at each position in the thermal block using a light meter with a small detector bulb to fit into the round holes drilled to fit the experimental bottles (LI-250A light meter, LI-COR). During measurements the detector bulb was positioned identically in each position, and if necessary, the positions of the fluorescent lights were adjusted nearer or farther until the light intensity was between 175-185 µmol photons m^{-2} s^{-1} for every experimental replicate.

Semi-continuous culturing methods were used for all experiments. Cultures were diluted with Aquil medium every two days to keep them in exponential growth stage while acclimating to the treatment temperatures for two weeks before starting the variation experiment. Dilution volumes were calculated to match growth rates of each individual replicate, as measured using *in vivo* chlorophyll a (Chl *a*) fluorescence. Once steady-state growth rates were recorded for 3–5 consecutive transfers, the cultures were sampled (Zhu et al., 2017). Due to the decrease of cell numbers during cultivation at 28.6 °C (from our preliminary experiment), these cultures were diluted from 22 °C stock cultures. They were then sampled as a batch culture (without dilution) after 4-6 days to estimate the negative growth rates and elemental stoichiometry at this

upper limit temperature point.

Six treatments were used to determine the responses of *E. huxleyi* growth, photosynthesis and calcification to different frequencies of temperature fluctuation. Temperature fluctuation treatments included: 1) Low temperature, constant (18.5 ^{o}C). 2) Low temperature, one-day fluctuation cycle (16-21^{o}C, mean = 18.5^{o}C). 3) Low temperature, two-day fluctuation cycle (16-21^{o}C, mean =18.5^{o}C). 4) High temperature, constant (25.5 ^{o}C). 5) High temperature, one-day fluctuation cycle (23-28^{o}C, mean = 25.5^{o}C). 6) High temperature, two-day fluctuation cycle (23-28^{o}C, mean = 25.5^{o}C). For the variation treatment cycles, cultures were incubated at the cool phase (16 ^{o}C and 23 ^{o}C for low and high temperatures, respectively) for either one or two days. They were then switched to the warm phase (21 ^{o}C and 28 ^{o}C for low and high temperature, respectively) for the same amount of time. It took about 1/2 hour to re-adjust the thermal block to the transformed temperature at the beginning of each new treatment cycle. The experimental *E. huxleyi* cultures were grown in triplicate in 120 ml acid washed polycarbonate bottles using the thermal-block under a 12 h light /12h dark cycle at 180 µmol photons m^{-2} s^{-1}.

For the variable temperature experiment, cultures were diluted semi-continuously with Aquil medium every two days for constant and one-day variation treatments, and every four days for two-day variation treatments. To ensure nutrient-replete conditions in the two-day variation treatments, Aquil nitrate and phosphate stocks were added at the two-day midpoint of every four days thermal cycle to make sure that the final nitrate and phosphate concentrations were not depleted and were always maintained

at >100 μmol L^{-1} and >10 μmol L^{-1}, respectively. Cultures were grown for at least eight dilutions (~16 days for constant and one day variation treatments; ~32 days for two-day variation treatments) to acclimate to the different experimental conditions before final sampling. All variation treatments were sampled twice across the thermal variation cycle, once during the cool phase and once during the warm phase.

Growth rates

In vivo fluorescence was measured daily for the one-day variation treatment and every two days for the constant and two-day variation treatments using a Turner 10-AU fluorometer (Turner Designs, CA). *In vivo*-derived growth rates were subsequently verified using cell samples counted with a nanoplankton counting chamber on an Olympus BX51 microscope. Specific growth rates (d^{-1}) were calculated using the *in vivo* fluorescence and cell count data as: $\mu=\ln[N(T_2)/N(T_1)]/(T_2-T_1)$, in which $N(T_1)$ and $N(T_2)$ are the *in vivo* fluorescence values (for thermal curve experiments and constant treatments) or cell counts (for variation treatments, because of potential changes in cellular *in vivo* fluorescence during fluctuation) at T_1 and T_2.

Chl *a* analysis

Twenty ml culture samples were filtered onto GF/F glass fiber filters (Whatman, Maidstone, UK) for Chl *a* analysis. In vitro Chl *a* was extracted with 90% aqueous acetone for 24 hours at -20 ^{o}C, and then measured using a Turner 10-AU fluorometer (Turner Design, USA). (Fu et al., 2007).

Elemental analysis

Elemental composition sampling included total particulate carbon (TPC),

particulate organic carbon (POC), particulate organic nitrogen (PON), particulate inorganic carbon (PIC) and particulate organic phosphorus (POP), allowing calculation of cellular elemental stoichiometry and calcite/organic carbon ratios (PIC/POC) (Feng et al.; 2008). Culture samples for TPC, POC and PON, were collected onto pre-combusted GF/F glass fiber filters (Whatman) and dried in a 60 ^{o}C oven overnight. For POC analysis, filters were fumed for 24 hours with saturated HCl (~37%) to remove all inorganic carbon prior to analysis. TPC, PON and POC were then measured by a 440 Elemental Analyzer (Costech Inc, CA) according to previous studies (Hutchins et al., 1998; Feng et al., 2008). PIC was calculated as the difference between TPC and POC. For POP measurement, culture samples were filtered onto pre-combusted GF/F filters (Whatman) and analyzed using a molybdate colorimetric method (Solórzano and Sharp, 1980), with minor modifications as in Fu et al. (2007).

Total carbon fixation, photosynthetic and calcification rates & ratios

Total carbon fixation, photosynthetic carbon fixation and calcification rates were measured using the ^{14}C incubation technique (Platt et al., 1980) with slight modifications as in Feng et al. (2008). Sixty mL culture samples from each treatment were spiked with 0.2 μCi $NaH^{14}CO_3$ and then incubated for 4 h under their respective experimental conditions. After incubation, samples were filtered on two Whatman GF/F filters (30mL each) for total carbon fixation and photosynthetic rate separately. The filters for photosynthetic rate measurement were fumed with saturated HCl (~37%) before adding scintillation fluid. Thirty mL from each treatment (10 mL from each

replicate bottle) was filtered immediately, after adding equal amounts of $NaH^{14}CO_3$ for procedural filter blanks. Filters were then placed in 7 mL scintillation vials with 4 mL scintillation fluid overnight in the dark. To determine the total radioactivity (TA), 0.2 µCi $NaH^{14}CO_3$ together with 100 µL phenylalanine was placed in scintillation vials with the addition of 4 mL scintillation solution. All samples were counted on a Perkin Elmer Liquid Scintillation Counter to measure the radioactivity. Total carbon fixation and photosynthetic rate were calculated from TA, final radioactivity and total dissolved inorganic carbon (DIC) values. Calcification rate was then calculated as the difference between total carbon fixation and photosynthetic rate for each sample.

Model for population growth of *E. huxleyi*

Growth rates measured under constant temperatures in the thermal block were fitted to the Eppley thermal performance curve (Eppley, 1972; Norberg, 2004; Thomas et al., 2012). This function quantifies parameters of growth temperature effects, including the temperature optimum for growth (T_{opt}), and high and low temperature limits (T_{max} and T_{min} respectively) in our strain of *E. huxleyi*. To predict growth rates under variable thermal regimes from our constant temperature thermal curves, we applied a recently developed model based on the Eppley curve, but incorporating non-linear averaging in conjunction with consideration of Jensen's inequality (Bernhardt et al., 2018). This new thermal fluctuation model takes into account the amount of time that the cells spend at each portion of their thermal performance curve, as well as incorporating the observation that growth rates usually increase slowly with temperature at the cooler end of the curve, but then drop off very quickly at the upper, warm end of the curve

(Jensen's inequality). This model is more realistic and skillful under variable temperatures than previous work assuming a linear relationship between temperature and growth rates, as non-linear averaging allows much more accurate predictions when dealing with skewed thermal curves. Several recent studies of phytoplankton thermal variability responses have successfully applied the Bernhardt et al. (2018) model (Qu et al. 2019, Kling et al. in press).

Statistical analysis

The mean values of most parameters measured under the variation treatments were calculated by averaging the values from the cool and warm phases, including all the elemental content and ratios, photosynthetic and calcification rates and ratios. Statistical analyses were performed using R (version 3.5.0). For the response of *E. huxleyi* to warming, the mean growth rate or elemental ratios of three replicates at 12 temperature points were used to fit the growth rate or elemental ratios curves. A one-way ANOVA was applied to analyze the difference between the average value for the entire temperature range and the value at each individual temperature for the elemental ratios. For the response of *E. huxleyi* to thermal variation, a one-way ANOVA was performed to test the statistical significance in growth rate, elemental stoichiometry, photosynthetic and calcification rates and ratios among different frequencies (constant, one-day and two-day) of temperature variabilities at cool/warm phases under high/low temperatures. *p*-values were calculated based on Student's t-test via two functions including compare_means() and stat_compare_mean() in the ggpubr package, and the figures were generated via the ggplot package in open source statistical software R

version 3.5.0 (R Foundation).

Results

Responses of *E. huxleyi* to warming

The growth rates of *E. huxleyi* at constant temperature increased significantly with warming from 0.09±0.01 d^{-1} at 8.5 ºC to a maximum value of 0.90±0.02 d^{-1} at 21.3 ºC. Growth was optimal up to 24.5 ºC, and then decreased rapidly to -0.46±0.05 d^{-1} at 28.6 ºC ($p<0.05$, Fig. 1).

The elemental ratios of the cells in the different temperature treatments were compared to the average elemental ratios across the entire temperature range (Fig. 2). The thermal trends of TPC/PON ratios were generally similar with those of growth rates, in that ratios increased from 8.5 to 17.5 ºC, and then decreased from 24.5 to 27.6 ºC. The TPC/PON ratios at 8.5, 10.5 and 27.6 ºC were significantly lower than the average level of all the temperature points ($p<0.05$, Fig 2A). The POC/PON ratios of most temperature points were very close to the mean value of 6.3, except at 27.6 ºC (7.1) and 28.6 ºC (7.4), which were significantly higher than the average ($p<0.05$, Fig 2B). The highest PIC/POC ratio was 0.49±0.07 at 22.6 ºC, and the lowest PIC/POC ratio was 0.05±0.04 at 27.6 ºC, a value that was almost 90% less than the highest value. The PIC/POC ratios at the lowest temperature tested (10.5 ºC) and at the high end of the temperature range (26.6 and 27.6 ºC) were significantly lower than the average level (Fig. 2C). Chl *a*/POC ratios were significant lower at 8.5, 10.5 and 27.6 ºC than the mean, and at 17.5, 21.3, 22.6 and 24.5 ºC were significantly higher than the average ($p<0.05$, Fig. 2C). The trends of PIC/POC and Chl *a*/POC ratio were similar, in that

282 they gradually increased from low temperature to the highest value at 22.6 ^{o}C, and
283 then dropped rapidly as temperature increased further. (Fig. 2C, D).

284 **Responses of *E. huxleyi* to temperature variations**

285 **Growth rate**

286 In low temperature experiments, both one-day and two-day temperature variations
287 had a negative effect on growth rate. The mean growth rates of the one-day (0.71±0.01
288 d^{-1}) and two-day (0.72±0.01 d^{-1}) variation treatments were not significantly different
289 from each other ($p>0.05$), but both were lower than that of the constant 18.5 ^{o}C
290 treatment (0.76±0.01, $p < 0.05$) (Fig. 3A). Growth rates were low during the cool phase
291 (16 ^{o}C) of the experiment (~0.5-0.6 d^{-1}), but those of the two-day variation cycle were
292 not significantly different from the constant control at this temperature ($p>0.05$).
293 However, the growth rates during the cool phase of the one-day variation cycle were
294 lower than those of the constant 16 ^{o}C treatment ($p<0.05$). During the warm phase of
295 the thermal cycle (21^{o}C), there were no significant differences in the elevated growth
296 rates (~0.85-0.9 d^{-1}) of the constant control and those of either variable treatment
297 ($p>0.05$, Fig. 3A).

298 In the high temperature experiments, as in the low temperature experiments, both
299 temperature variation frequencies had a negative effect on mean growth rates. The
300 growth rates in the two-day variation treatment were (0.20±0.02 d^{-1}), a decrease of
301 ~74% compared with the constant 25.5 ^{o}C ($p<0.05$), and ~62% of the one-day
302 variation treatment value ($p<0.05$, Fig. 3B). During the cool phase (23 ^{o}C), the growth
303 rate of the one-day variation treatment was slightly lower ($p<0.05$) than the constant

304 23 °C, but there were no significant changes between two-day variations and the
305 constant 23 °C treatment ($p > 0.05$, Fig. 3B). During the warm phase (28 °C), the
306 constant 28 °C and two-day variation treatment both had negative growth rates of -
307 0.45±0.05 d^{-1} and -0.45±0.04 d^{-1}, respectively. However, the one-day variation
308 treatment had a low but positive warm phase growth rate at 0.25±0.02 d^{-1} (Fig. 3B).
309 There was a time lag of ~1/2 hour to switch to the transformed temperature for each
310 new growth phase, which should thus have had only minimal effects on overall growth
311 rates across the one-day and two-day thermal variations.

312 **Cellular PIC and POC contents and ratios**

313 In low temperature experiments, the cellular PIC content of the constant 18.5 °C
314 treatment was 3.5±0.3 pg/cell, and there were no significant differences with
315 temperature variation treatments ($p> 0.05$, Table 1). However, the cellular POC
316 content of the constant 18.5 °C treatment was 8.0±0.6 pg/cell, which was lower than
317 in the two-day variation treatment, but significantly higher than in the one-day
318 variation treatment ($p<0.05$).

319 Like POC, the PIC/POC ratio was significantly affected by temperature variations
320 (Fig. 4A). The lowest PIC/POC ratio was found in the one-day variation treatment
321 (0.38 ±0.07), which was significantly lower than the two-day variation treatment value
322 ($p < 0.05$), but close to that in the constant 18.5 °C ($p > 0.05$). A similar trend was
323 found in both the cool (16 °C) and warm phases (21 °C) of the two variation treatments,
324 in that the PIC/POC ratio of the one-day variation treatment was lower than of the
325 two-day variation treatment ($p < 0.05$, Fig. 4A). Both variation treatments had lower

PIC/POC ratios during the warm phase than during the cool phase, although these differences were not significant ($p>0.05$).

High temperature experiments showed particulate carbon trends that were contrary to those of the low temperature treatments. The PIC content and PIC/POC ratios were significantly decreased by temperature variation. The cellular PIC content of the constant treatment (25.5 ^{o}C) was 5.5±0.3 pg/cell, which was ~ 200% higher than that of the one-day variation and ~ 160% higher than in the two-day variation treatments ($p<0.05$, Table 1). The same trend was found for PIC/POC ratios in one-day variation and two-day variation treatments, which decreased ~ 67% and 33% compared with the constant 25.5 ^{o}C treatment, respectively ($p<0.05$, Fig. 4B). However, the POC content of one-day and two-day variation treatments was higher than in the constant 25.5 ^{o}C treatment ($p < 0.05$,Table 1). During the cool phase (23 ^{o}C), the PIC content and PIC/POC ratio of the one-day variation treatment was significantly lower than in the two-day variation treatment, but contrary to PIC content, the POC content of the one-day variation treatment was significantly higher than that in the two-day variation treatment. During the warm phase (28 ^{o}C), there were no significant differences of PIC content, POC content, or PIC/POC ratio between the one-day and two-day variation treatments (Fig. 4B, Table 1).

Photosynthetic and calcification rates and ratios

In low temperature treatments, there were no differences between total carbon fixation rates (photosynthesis plus calcification) for the two variable treatments relative to the constant control (Fig. 5A). However, during the cool phase total

carbon fixation rates were higher in the one-day variation than in the two-day variation ($p<0.05$, Fig 5A), while this rate was the same in both variation treatments during the warm phase ($p > 0.05$, Fig. 5A). In high temperature experiments, the total carbon fixation rates of the one-day and two-day variation treatments were significantly decreased by about ~20% and ~18% respectively, compared with the constant 25.5 ^{o}C treatment ($p<0.05$, Fig. 5 B).

The photosynthetic and calcification rates of the constant 18.5 ^{o}C treatment were 0.04±0.00 pmol C cell^{-1} hr^{-1} and 0.02±0.00 pmol C cell^{-1} hr^{-1}, respectively, which were not significantly different from both of the temperature variation treatments ($p > 0.05$, Fig. 5 C,E). Photosynthetic rates changed within the thermal cycle for both one-day and two-day variation treatments, with a decrease of 22% and 28% from the warm phase to the cool phase, respectively (Fig. 5C). However, there were no significant changes in calcification rates under either variation frequency treatment between the cool and warm phases of the thermal cycles ($p > 0.05$).

In the mean 25.5 ^{o}C experiment, photosynthetic rates were not significantly different between the one-day variation and constant treatments ($p > 0.05$), while the photosynthetic rate of the two-day variation was slightly higher than that of the constant 25.5 ^{o}C treatment ($p<0.05$, Fig. 5D). In contrast, calcification rates of one-day and two-day variation treatments at a mean temperature of 25.5 ^{o} were significantly decreased by about ~46% and ~51%, respectively, relative to the constant control ($p<0.05$, Fig. 5F). There were no significant differences in total carbon fixation, photosynthetic and calcification rates between the one-day variation and two-day

variation treatments during both the cool (23 ^{o}C) and warm (28 ^{o}C) phases ($p>0.05$, Fig. 5 B,D,F).

In the low temperature treatments, there were no significant differences in calcification to photosynthesis (Cal/Photo) ratios between the constant and the two variable treatments ($p > 0.05$, Fig 6A). In contrast, in the high temperature experiments, the Cal/Photo ratio of the one-day variation and two-day variation treatments were decreased by ~40% and 49%, respectively, compared with the constant 25.5 ^{o}C treatment ($p<0.05$, Fig. 6B). For both low and high temperature experiments, there were no significant differences between the one-day and two-day variation treatments in either the cool or warm phases of the thermal cycle ($p > 0.05$, Fig. 6B). However, in both temperature treatments the lower photosynthetic rates during the cool phase (Fig. 5C,D) resulted in an increase in the Cal/Photo ratio during the cool phase for both the one-day and two-day variation treatments ($p<0.05$ Fig. 6A,B).

Elemental content and stoichiometry

In the low temperature experiments, the one-day variation and two-day thermal variations had different effects on cellular elemental contents and ratios, relative to the constant 18.5 ^{o}C treatment. One-day variation increased most of the cellular elemental and biochemical contents (TPC, PON, and Chl *a*) but with no significant difference ($p>0.05$), except for POP content ($p<0.05$), compared with the constant 18.5 ^{o}C treatment (Table 1). In contrast, the two-day variation treatment decreased all the measured cellular elemental and biochemical contents (TPC, PON, POP and Chl *a*,

392 $p<0.05$) in relation to the constant 18.5 ^{o}C treatment (Table 1). However, the
393 TPC/PON and Chl *a*/POC ratios of the two-day variation treatment were higher than
394 those of the one-day variation and constant 18.5 ^{o}C treatments ($p<0.05$, Fig. 7A,E),
395 while the PON/POP ratio was lower than in the one-day variation and constant 18.5
396 ^{o}C treatments ($p<0.05$, Fig. 7C). There were no significant differences in TPC/PON,
397 PON/POP and Chl *a*/POC ratios between the constant 18.5 ^{o}C and the one-day
398 variation treatments ($p > 0.05$, Fig. 7A).

399 In high temperature experiments, the highest cellular TPC, PON and POP contents
400 were all obtained under the one-day variation treatment, which was significantly
401 higher than under constant 25.5 ^{o}C conditions ($p<0.05$, Table 1). However, there were
402 no significant differences in cellular Chl *a* content between the constant 25.5 ^{o}C and
403 both variation treatments ($p > 0.05$, Table 1). The TPC/PON ratio of the constant 25.5
404 ^{o}C treatment was ~22% and ~35% higher than that of the two-day variation and one-
405 day variation treatments, respectively ($p<0.05$, Fig. 7B), while the PON/POP ratio was
406 highest in the one-day variation, followed by the two-day variation and finally by the
407 constant control (Fig. 7D). The Chl *a*/POC ratio of the one-day variation treatment
408 was significantly lower than that of the constant 25.5 ^{o}C and two-day variation
409 treatments ($p<0.05$), but there were no significant differences between the constant
410 25.5 ^{o}C and two-day variation treatments ($p > 0.05$, Fig. 7F).

411 During the cool phase of the high temperature experiments (23 ^{o}C), the cellular
412 TPC, PON, POP and Chl *a* content of two-day variation were all significantly lower
413 than in the one-day variation treatment ($p<0.05$). Similar decreasing trends during the

414 cool phase were observed for the TPC/PON ratios (Fig. 7B), but not the Chl *a*/POC
415 ratio, which was ~32% higher than in the one-day variation treatment ($p<0.05$, Fig.
416 7F). During the warm phase (28 ^{o}C), there were no significant differences of cellular
417 TPC, PON and POP contents between one-day and two-day variation treatments ($p >$
418 0.05, Table 1) as well as the TPC/PON ratio (Fig 7B). However, the Chl *a* content of
419 the one-day variation treatment was ~20% lower than that of the two-day variation
420 treatment ($p<0.05$). The Chl *a*/POC ratio was not significantly different between the
421 one-day and two-day variation treatments at the warm phase ($p > 0.05$, Table 1, Fig.
422 7F).

423 **Experimental constant temperature performance curves and measured and**
424 **modeled fluctuating temperature performance curves**

425 The experimentally-determined constant condition temperature performance
426 curves and the predicted fluctuating temperature condition temperature performance
427 curves based on the Bernhardt et al. (2018) non-linear averaging model are shown in
428 Fig. 8 for *E. huxleyi*. Compared with the measured temperature performance curve
429 under constant thermal conditions, the modeled curve of the fluctuating temperature
430 condition showed a leftward shift towards lower temperatures at optimum
431 temperatures and above. The maximum and optimal temperature of the modeled
432 fluctuating temperature performance curve were all lower than those of the measured
433 constant condition curve. In particular, the optimal temperature for growth decreased
434 from 22^{o}C in constant conditions to 21 ^{o}C under fluctuating temperature conditions.
435 At the same time, the maximum growth rate (μ_{max}) of the fluctuating temperature

condition was 0.8 d^{-1}, which was lower than the constant condition value of 0. 9 d^{-1}. The measured growth rates of experimental one-day (0.71 d^{-1}) and two-day (0.72 d^{-1}) variation treatments at the relatively low mean temperature of 18.5 ^{o}C closely matched the model-predicted fluctuating temperature growth rate at this temperature (0.74^{-1}, Fig. 8). However, measured and predicted growth rates did not match as well at the higher mean temperature. At 25.5 ^{o}C, the measured growth rate of the one-day variation was 0.52 d^{-1}, 30% higher than the predicted fluctuating temperature growth rate of 0.40 d^{-1}. In contrast, the measured growth rate of the experimental two-day variation treatment was 0.20 d^{-1}, a decrease of 50% compared to the model-predicted fluctuating temperature growth rate of 0.40 d^{-1} at this temperature (Fig. 8).

Discussion

Effects of warming on *Emiliania huxleyi* growth rates and elemental ratios

Thermal response curves and optimum growth temperatures describe the importance of temperature as a control on the distribution of *E. huxleyi* strains in the ocean (Buitenhuis et al., 2008; Paasche, 2001). The optimal temperature range of 21.3-24.5 ^{o}C found in our study is similar to that of some other *E. huxleyi* strains (De Bodt et al., 2010; Feng et al., 2017; Rosas-Navarro et al., 2016; Zhang et al., 2014). Most studies have focused on the lower part of the temperature curve where growth rates increase with rising temperatures (Feng et al., 2017; Matson et al., 2016), with relatively few examining stressfully warm temperatures where growth is inhibited (Zhang et al., 2014).

In our study, the descending portion of the upper temperature performance curve

458 ranged from 24.5 °C to 28.6 °C, at which point growth rates became negative. We
459 repeated the upper thermal limit part of the curve several times to rigorously verify that
460 cultures were unable to grow at this temperature. The magnitude of the negative growth
461 rate is presented here as it represents an expression of the degree of stress the culture
462 experienced at this temperature, and so makes a useful comparison with the other
463 positive growth rate values in the variation experiments. This *E. huxleyi* strain was
464 isolated from the Sargasso Sea where the sea surface temperature can reach 29 °C in
465 the summer, and will undoubtedly be higher in the future with global warming
466 (https://seatemperature.info/sargasso-sea-water-temperature.html). This suggests that
467 this strain may be currently living at or very near its upper thermal limit for part of the
468 year, as are many other tropical and subtropical phytoplankton (Thomas et al. 2012),
469 and that it may therefore be vulnerable to further warming.

470 Calcification is the key biogeochemical functional trait of this species, and the
471 PIC/POC ratio of *E. huxleyi* can be influenced by factors that include CO_2 concentration,
472 nutrient status, irradiance and temperature (Feng et al., 2008, 2017; Raven & Crawfurd,
473 2012). The cellular PIC/POC of *E. huxleyi* has been reported to decrease as irradiance
474 and CO_2 concentration rise, but to increase under nitrate and phosphate limitation (Feng
475 et al., 2017; Paasche, 1999; Riegman et al., 2000). The effect of temperature on *E.*
476 *huxleyi* cellular PIC/POC ratio is however more complex. De Bodt et al. (2010) and
477 Gerecht et al. (2014) observed that higher cellular PIC/POC ratios were obtained at
478 lower temperatures for both *E. huxleyi* and *Coccolithus pelagicus*. Sett et al. (2014),
479 however, found an opposite trend, whereby the PIC/POC ratio increased with

480 temperature in another strain of *E. huxleyi*. Feng et al. (2017) reported that the cellular
481 PIC/POC of *E. huxleyi* was increased as the temperature rose from 4 ^{o}C to 11 ^{o}C, but
482 decreased with warming from 11 ^{o}C to 15 ^{o}C and remained steady afterwards.

483 In our study, the cellular PIC/POC ratio of *E. huxleyi* was positively correlated to
484 growth rate (R^2=0.73), and increased with warming from 8.5 ^{o}C to a maximum at 22.6
485 ^{o}C, and then decreased with further warming to 27.6 ^{o}C. In a meta-analysis of studies
486 using different coccolithophore subgroups, Krumhardt et al. (2017) found that the
487 highest PIC/POC ratios were observed between 15 °C and 20 °C, in the same thermal
488 range where the highest growth rates of *E. huxleyi* are found, as seen here and in Sett
489 et al. (2014). In contrast, Rosas-Navarro et al. (2016) reported that the cellular PIC/POC
490 ratio showed a minimum at optimal growth temperature (between 20 and 25 °C) for
491 three strains of *E. huxleyi*. However, the *E. huxleyi* strain used here was isolated from
492 a warmer area (the Sargasso Sea) compared with isolates from coastal Japan and New
493 Zealand in previous studies (Rosas-Navarro et al. 2016; Feng et al. 2017). The growth
494 temperature for our stock cultures was 22-24^{o}C, higher than that of the other two *E.*
495 *huxleyi* strains. Feng et al. (2017) also found that the optimal temperature for
496 calcification was close to the stock culture maintenance temperature in their study.

497 Our results also support suggestions that stressful high temperatures may lead to
498 decreases in cellular PIC/POC ratios and calcification (De Bodt et al., 2010; Feng et al.,
499 2017; Gerecht et al., 2014; Krumhardt et al., 2017). The cellular PIC/POC ratio of *E.*
500 *huxleyi* was much more plastic than the other ratios we measured, including TPC/PON
501 and POC/PON. Indeed, PIC/POC ratios may change dramatically (>2-fold) with

temperature for some coccolithophore subgroups (Krumhardt et al., 2017). The plasticity in PIC/POC ratios of *E. huxleyi* during temperature changes in our study may have implications for shifts in the ballasting of coccolith-containing particles during sinking, thus affecting the ocean carbon cycle.

The cellular Chl *a*/POC ratio of *E. huxleyi* showed a similar pattern with the PIC/POC ratio, as it was also positively correlated to growth rate. Zhu et al. (2017) reported the cellular Chl *a*/POC ratio of a Southern California diatom was also correlated to growth rate across a very similar temperature range. In contrast, Feng et al. (2017) found that the cellular Chl *a*/POC ratio of *E. huxleyi* dramatically decreased with warming. However, in our experiments, the cellular Chl *a*/POC ratio was lower at 27.6 ^{o}C than at 28.6 ^{o}C, likely due to the negative growth rates and consequent lack of acclimation of the cultures maintained at the highest temperature. Traits such as PIC/POC ratios, Chl *a*/POC ratios and TPC/PON ratios also showed some evidence for possible carryover from the stock cultures (22-24 ^{o}C) in this 28.6 ^{o}C treatment, as we were forced to sample before the cells died completely, after only 2-3 cycles of dilution.

Effect of thermal variation on *Emiliania huxleyi* growth and physiology

Constant vs variable temperature

Thermal variability in the surface ocean is becoming an increasingly relevant topic as global warming proceeds. In our study, we found that the growth rates of a subtropical *E. huxleyi* strain were quite sensitive to temperature variation under both low (18.5 ^{o}C, “winter”) and high (25.5 ^{o}C, “summer”) mean temperatures. In both low and high temperature experiments, growth rates always decreased under temperature

524 variation, compared with the constant mean temperature. This result agrees with
525 previous studies showing that temperature variation slowed the growth rates of the
526 fresh water green alga *Chlorella pyrenoidosa* and the marine diatom *Cyclotella*
527 *meneghiniana*, as observed in laboratory work but also during long-term field
528 observations (Zhang et al., 2016).

529 This growth rate inhibition under temperature variation was more pronounced at
530 high temperature than at low temperature, indicating that variability at the warm range
531 boundary will have a stronger negative effect on population growth rate than
532 variability near the lower thermal limits (Bernhardt et al., 2018). This trend suggests
533 that acclimation to high temperature (whether constant or variable) may require greater
534 investment in cellular repair machinery, such as heat shock proteins, thus potentially
535 diverting nutrient and energy supplies and thereby reducing growth rates (O'Donnell
536 et al., 2018). However, following Jensen's inequality model to predict the thermal
537 performance curve, there should be an inflection point where the transfer between
538 positive and negative effects of temperature variability will occur compared with the
539 constant thermal curve. Conversely, for phytoplankton living in regions of suboptimal
540 temperatures, thermal variation can enhance growth (Bernhardt et al., 2018). Thus, for
541 some polar phytoplankton or for temperate species extending their ranges poleward,
542 such as *E. huxleyi* (Neukermans et al., 2018), not only warming but also thermal
543 variability may need to be taken into consideration in order to understand changes in
544 high latitude microbial communities and biogeochemistry cycles.

545 Temperature variation affected the physiology of *E. huxleyi* differently compared

546 with constant temperature. Physiological traits that were affected by thermal
547 fluctuations also differed at low temperature ("winter") and high temperature
548 ("summer"), suggesting different response mechanisms. Under low temperature
549 variations (16-21 ^{o}C), photosynthesis and calcification were correlated with
550 temperature, leading to rates similar to those observed with constant temperature.
551 However, elemental contents and ratios under thermal variations differed from
552 constant temperature. For instance, the cellular POC, PON, POP and Chl *a* contents
553 increased during one-day variations but decreased during two-day variations,
554 compared with constant temperature.

555 These cellular quota changes were reflected in elemental ratio differences
556 (PIC/POC, Chl a/POC and TPC/POC) between the thermal variation treatments and
557 constant temperature. However, the changes between thermal variation and constant
558 treatments were not significant under low temperature ("winter"), indicating that the
559 thermal variation wouldn't significantly influence biogeochemical cycles under these
560 conditions. Unlike constant temperature treatments where selection may favor a higher
561 growth rate, the trade-off for the thermal variation treatments may involve sacrificing
562 increased growth rate in order to adjust cellular stoichiometry to adapt to the
563 fluctuating environment.

564 In contrast, photosynthetic and calcification rates under high temperature thermal
565 variations (23-28 ^{o}C) were significantly different from those seen under constant
566 temperature (25 ^{o}C), especially the calcification rate. Thermal variation treatments
567 transiently but repeatedly experienced the extreme high temperature point (28 ^{o}C),

568 leading to extremely low calcification rates and PIC contents, and thus relatively low
569 PIC/POC and Cal/Photo ratios. Previous *E. huxleyi* studies agree that high temperature
570 decreases PIC content, PIC/POC ratios and Cal/Photo ratios (Feng et al., 2017; 2018;
571 Gerecht et al., 2014). The two different patterns of responses to thermal variation we
572 observed under low and high temperatures imply a seasonal pattern in the ways that
573 thermal variations will affect the elemental stoichiometry of *E. huxleyi* .

574 Under other stresses such as nutrient limitation, trade-offs between growth rates
575 and resource affinities may be necessary to adapt to thermal changes. For instance,
576 nitrate affinity declines in cultures of the large centric diatom *Coscinodiscus*
577 acclimated to warmer temperatures (Qu et al. 2018), while warming decreases cellular
578 requirements for iron in the nitrogen-fixing cyanobacterium *Trichodesmium* (Jiang et
579 al. 2018). In nitrogen-limited cultures of the marine diatom *Thalassiosira pseudonana*,
580 long-term thermal adaptation acted most strongly on systems other than those involved
581 in nitrate uptake and utilization (O'Donnell et al., 2018). Thus, it is possible that our
582 thermal response results with *E. huxleyi* might have differed under nutrient-limited
583 growth conditions.

584 ***One-day vs two-day thermal variation***

585 As temperature fluctuations in the surface ocean increase along with climate
586 change, phytoplankton will be influenced by the frequencies and intensities of these
587 thermal excursions. We found that the responses of *E. huxleyi* to one-day versus two-
588 day temperature variations were different at both low and high temperature. For
589 instance, under low temperature the transition from the warm phase to the cool phase

590 during the thermal variation could be treated as a low temperature stress leading to a
591 lag phase in growth. The growth rate of the one-day variation treatment at the cool
592 phase was lower than that of the two-day variation, suggesting that physiological
593 acclimation is not rapid enough to accommodate to the shorter variation treatment,
594 while the two-day variation allows enough time for growth to recover. However, at
595 the warm phase (21 ^{o}C) there was no difference in growth rates between the one-day
596 and two-day variations compared with the constant 21-degree treatment. These results
597 imply that there was a shorter lag phase after transfer at the optimal temperature point
598 (21 ^{o}C at the warm phase) than during low temperature stress (16 ^{o}C at the cool phase).
599 There was no significant difference in photosynthetic rates between the one-day
600 and two-day variation during the warm phase (21 ^{o}C), but both were higher than during
601 the cool phase, indicating the photosynthetic rate was correlated to the thermal
602 variation cycle. However, for the calcification rate there was no significant difference
603 between one-day and two-day variations during either the cool or warm phases. These
604 results suggested that photosynthesis was more responsive to temperature variations
605 than calcification, and so ultimately determined the growth rate in both cool and warm
606 phases. Feng et al. (2017) reported a similar relationship between growth and
607 photosynthetic rates of a Southern Hemisphere *E. huxleyi* strain cultured at different
608 temperatures.
609 Temperature variation frequencies also strongly influenced elemental
610 composition. In low temperature experiments, the cellular contents of PON, POP and
611 POC in the one-day variation treatment were all higher than under two-day variations.

612 A notable exception to this trend was the cellular PIC content, which was not
613 significantly different between one-day and two-day variation treatments. The PIC
614 content was positively correlated to calcification and relatively stable, indicating that
615 coccolith production and storage of *E. huxleyi* was relatively independent of the
616 frequency of thermal variation.

617 Unlike the photosynthetic rate, the cellular elemental content of one-day and two-
618 day variations were significantly different, but were not changed during temperature
619 variation when transitioning from the warm phase to the cool phase or vice versa.
620 The temperature dependent photosynthetic enzyme activity likely determined the
621 similar photosynthetic rate of one-day and two-day variation treatments at both cool
622 and warm phase in our short-term experiment, but the divergent responses of cellular
623 stoichiometry in one-day and two-day thermal variations indicated different
624 mechanisms of rapid acclimation to different thermal fluctuation frequencies. Our
625 results imply that the responses of *E. huxleyi* to one-day and two-day thermal
626 variations have different patterns, but both reach stable states during extended periods
627 of temperature fluctuation. Due to decreasing POC content, the PIC/POC ratio
628 increased in the two-day variation compared with the one-day variation, suggesting
629 that more rapid thermal fluctuations might lead to a decrease in calcite ballasting of
630 sinking organic carbon.

631 Under the high temperature scenario, thermal variation forces the microalgae to
632 intermittently deal with a lethal high temperature during the warm phase (28 ^{o}C), with
633 potentially irreversible damage to the cells. In the “summer” experiments, the mean

growth rate of the two-day variation was much lower than that of the one-day variation. This mainly resulted from the negative growth rate of two-day variation cultures during the warm phase (28 ^{o}C), whereas the growth rate of the one-day variation was >0.20 d^{-1}. This result demonstrates that high frequency temperature variations (one-day) can partly mitigate growth inhibition by high temperatures in *E. huxleyi*, and so allow tolerance to extreme thermal events relative to longer exposures. This observation agrees with previous studies of other marine organisms such as corals (Oliver & Palumbi, 2011; Safaie et al., 2018). In the case of our experiments, the lag phase and metabolic inertia would help to maintain the microalgae during short exposures (one-day) to high temperature when transitioning from the cool phase (23 ^{o}C) to the warm phase (28 ^{o}C).

Likewise, the particulate organic element contents (PON, POP and POC) of *E. huxleyi* were more stable in one-day than in two-day temperature variation treatments. The relatively steady status of cellular particulate organic matter content in the high frequency temperature variation treatment may conserve energy, compared to the energy-intensive redistribution of major cellular components under lower frequency temperature variations. This differential energetic cost may help to explain the differences in growth rates between the two treatments. Adaptation to high temperature may also require higher investment in repair machinery, such as heat shock proteins, leading to an increased demand for nitrogen and other nutrients, thus increasing cellular POC, PON and POP contents (O'Donnell et al., 2018).

Prediction and modelling of *E. huxleyi* responses to thermal variation

Mathematical curves based on population growth rates from laboratory studies have been used to predict future population abundance, persistence or fitness in a changing world (Bernhardt et al., 2018; Deutsch et al., 2008; Jiang et al. 2017). We applied a modified version of the Eppley thermal performance curve model with the addition of non-linear averaging (Bernhardt et al., 2018) to predict the influence of thermal variation on the growth rate of *E. huxleyi* (Fig. 8). *E. huxleyi* growth rates were predicted to be much lower at warmer temperatures under variable conditions compared to constant conditions, but there were no significant differences at cooler temperatures. Thus, the effect of thermal variation on population growth at the upper thermal limit was predicted to be stronger than that in the lower portion of the thermal range (Bernhardt et al., 2018; Sunday et al., 2012). This phenomenon has been widely observed in ectothermic animal taxa (Dell et al., 2011), but this model for the effect of thermal variation on population growth rate may lack the ability to predict species responses at the extreme edges of their ranges (Bernhardt et al., 2018).

Our results showed that the measured effects of a variable thermal regime on *E. huxleyi* growth rate fitted well with model-predicted values at a relatively low temperature (mean=18.5 ^{o}C), but differed considerably at high temperature (mean=25.5 ^{o}C). This was especially evident under the two-day variation conditions at a mean of 25.5 ^{o}C, where the growth rate was sharply lower than predicted from the constant temperature performance curve-based model. This result suggests that transient heat waves may erode thermal tolerances of *E. huxleyi* populations already growing near their upper thermal limits, and that the frequency and duration of such extreme events

678 is critically important in determining the magnitude of this stress. Qu et al. (2019)
679 reported that the tropical cyanobacterium *Trichodesmium erythraeum* only showed a
680 slight decrease of growth rate with thermal variation treatments at high temperature
681 (average 30^{o}C), compared with constant 30^{o}C treatments. In contrast, the sensitivity of
682 this *E. huxleyi* isolate to increasing thermal variability may reduce its fitness and its
683 ability to compete with other taxa such as diatoms and cyanobacteria, with implications
684 for community structure in the future sub-tropical ocean.

685 Although thermal variation at high temperature negatively impacted the growth
686 rate of *E. huxleyi* in our experiment, our relatively short-term study did not address the
687 potential for *E. huxleyi* to evolve under selection by frequent extreme heat events.
688 Evolutionary change in the thermal optimum and the maximum growth temperature in
689 response to ocean warming may reduce heat-induced mortality, and mitigate some
690 ecological impacts of global warming (O'Donnell et al., 2018, Thomas et al., 2012). For
691 example, Schlüter et al. (2014) found that after one year of experimental adaptation to
692 warming (26.3°C), the marine coccolithophore *E. huxleyi* evolved a higher growth rate
693 when assayed at the upper thermal tolerance limit. Similar results were reported for the
694 marine diatom *Thalassiosira pseudonana* in recent studies (O'Donnell et al., 2018;
695 Schaum et al., 2018). Schaum et al. (2018) also found that the evolution of thermal
696 tolerance in marine diatoms can be particularly rapid in fluctuating environments.
697 Furthermore, populations originating from more variable environments are generally
698 more plastic (Schaum & Collins, 2014; Schaum et al., 2013). Long-term evolutionary
699 experiments with *E. huxleyi* will be necessary to determine how the thermal

performance curve of this important marine calcifier may diverge under selection by different frequencies and durations of extreme thermal variation events.

Understanding the combination of ocean warming and magnified thermal variability may be a prerequisite to accurately predicting the effects of climate change on the growth and physiology of the key marine calcifier *E. huxleyi.* This information will help to inform biogeochemical models of the marine and global carbon cycles, and ecological models of phytoplankton distributions and primary productivity. How changing thermal variation frequencies and heat wave events will affect marine phytoplankton remains a relatively under-explored topic, but one that is likely to become increasingly important in the future changing ocean.

Data availability

The data are available by request from the corresponding author (DAH), and at www.bco-dmo.org/project/668547.

Author contributions

XW, F-XF and DAH contributed to conceiving and planning the experiments. XW, F-XF, PQ, JDK, and H-BJ performed the lab experiments. XW, F-XF, Y-HG and DAH contributed to the data analysis and to writing the paper. All of the authors contributed comments, revisions and editing.

Competing interests

The authors declare that they have no conflict of interest.

Acknowledgements

Support was provided by the U.S. National Science Foundation Biological Oceanography grants OCE1538525 and OCE1638804 to F-XF and DAH, National Key Research and Development Program of China 2016YFA0601302 to Y-HG. XW was supported by a grant from the China Scholarship Council. We would like to thank the two reviewers for their constructive comments and suggestions.

730 **References**

731 Bernhardt, J. R., Sunday, J. M., Thompson, P. L., and O'Connor, M. I.: Nonlinear
732 averaging of thermal experience predicts population growth rates in a thermally
733 variable environment, bioRxiv, 247908, 2018.

734 Boyce, D. G., Lewis, M. R., and Worm, B.: Global phytoplankton decline over the past
735 century, https://doi.org/10.1038/nature09268, Nature, 466, 591, 2010.

736 Boyd, P., Dillingham, P., McGraw, C., Armstrong, E., Cornwall, C., Feng, Y.-y., Hurd,
737 C., Gault-Ringold, M., Roleda, M., and Timmins-Schiffman, E.: Physiological
738 responses of a Southern Ocean diatom to complex future ocean conditions, Nature
739 Climate Change, 6, 207-216, https://doi.org/10.1038/nclimate2811, 2015.

740 Boyd, P. W., Strzepek, R., Fu, F., and Hutchins, D. A.: Environmental control of open-
741 ocean phytoplankton groups: Now and in the future, Limnol. Oceanogr., 55, 1353-
742 1376, https://doi.org/10.4319/lo.2010.55.3.1353, 2010.

743 Boyd, P. W., Collins, S., Dupont, S., Fabricius, K., Gattuso, J. P., Havenhand, J.,
744 Hutchins, D. A., Riebesell, U., Rintoul, M. S., and Vichi, M.: Experimental
745 strategies to assess the biological ramifications of multiple drivers of global ocean
746 change—A review, Glob. Chang. Biol., 24, 2239-2261,
747 https://doi.org/10.1111/gcb.14102, 2018.

748 Bozinovic, F., Bastías, D. A., Boher, F., Clavijo-Baquet, S., Estay, S. A., and Angilletta
749 Jr, M. J.: The mean and variance of environmental temperature interact to
750 determine physiological tolerance and fitness, Physiol. Biochem. Zool., 84, 543-
751 552, https://doi.org/10.1086/662551, 2011.

752 Buitenhuis, E. T., Pangerc, T., Franklin, D. J., Le Quéré, C., and Malin, G.: Growth
753 rates of six coccolithophorid strains as a function of temperature, Limnol.
754 Oceanogr., 53, 1181-1185, https://doi.org/10.4319/lo.2008.53.3.1181, 2008.
755 Burgmer, T., and Hillebrand, H.: Temperature mean and variance alter phytoplankton
756 biomass and biodiversity in a long-term microcosm experiment, Oikos, 120, 922-
757 933, https://doi.org/10.1111/j.1600-0706.2010.19301.x, 2011.
758 Cáceres, C. E.: Temporal variation, dormancy, and coexistence: a field test of the
759 storage effect, Proceedings of the National Academy of Sciences, 94, 9171-9175,
760 https://doi.org/10.2307/42576, 1997.
761 De Bodt, C., Van Oostende, N., Harlay, J., Sabbe, K., and Chou, L.: Individual and
762 interacting effects of pCO_2 and temperature on *Emiliania huxleyi* calcification:
763 study of the calcite production, the coccolith morphology and the coccosphere size,
764 Biogeosciences, 7, 1401-1412, https://doi.org/10.5194/bg-7-1401-2010, 2010.
765 Dell, A. I., Pawar, S., and Savage, V. M.: Systematic variation in the temperature
766 dependence of physiological and ecological traits, Proceedings of the National
767 Academy of Sciences, 108, 10591-10596, https://doi.org/10.2307/27978658, 2011.
768 Deutsch, C. A., Tewksbury, J. J., Huey, R. B., Sheldon, K. S., Ghalambor, C. K., Haak,
769 D. C., and Martin, P. R.: Impacts of climate warming on terrestrial ectotherms
770 across latitude, Proceedings of the National Academy of Sciences, 105, 6668-6672,
771 https://doi.org/10.1073/pnas.0709472105, 2008.
772 Eppley, R. W.: Temperature and phytoplankton growth in the sea, Fish. Bull, 70, 1063-
773 1085, 1972.

774 Feng, Y., Warner, M. E., Zhang, Y., Sun, J., Fu, F.-X., Rose, J. M., and Hutchins, D. A.:
775 Interactive effects of increased pCO_2, temperature and irradiance on the marine
776 coccolithophore *Emiliania huxleyi* (Prymnesiophyceae), Eur. J. Phycol., 43, 87-98,
777 https://doi.org/10.1080/09670260701664674, 2008.
778 Feng, Y., Roleda, M. Y., Armstrong, E., Boyd, P. W., and Hurd, C. L.: Environmental
779 controls on the growth, photosynthetic and calcification rates of a Southern
780 Hemisphere strain of the coccolithophore *Emiliania huxleyi*, Limnol. Oceanogr.,
781 62, 519-540, https://doi.org/10.1002/lno.10442, 2017.
782 Feng, Y., Roleda, M. Y., Armstrong, E., Law, C. S., Boyd, P. W., and Hurd, C. L.:
783 Environmental controls on the elemental composition of a Southern Hemisphere
784 strain of the coccolithophore *Emiliania huxleyi*, Biogeosciences, 15, 581-595,
785 https://doi.org/10.1002/lno.10442, 2018.
786 Friedland, K. D., Mouw, C. B., Asch, R. G., Ferreira, A. S. A., Henson, S., Hyde, K. J.,
787 Morse, R. E., Thomas, A. C., and Brady, D. C.: Phenology and time series trends
788 of the dominant seasonal phytoplankton bloom across global scales, Global Ecol.
789 Biogeogr., 27, 551-569, https://doi.org/10.1111/geb.12717, 2018.
790 Fu, F.-X., Yu, E., Garcia, N. S., Gale, J., Luo, Y., Webb, E. A., and Hutchins, D. A.:
791 Differing responses of marine N_2 fixers to warming and consequences for future
792 diazotroph community structure, Aquat. Microb. Ecol., 72, 33-46,
793 https://doi.org/10.5194/bgd-12-4273-2015, 2014.
794 Fu F.-X., Tatters A.O., and Hutchins, D.A.: Global change and the future of harmful
795 algal blooms in the ocean. Marine Ecology Progress Series 470: 207-233 DOI:

796 10.3354/meps10047, 2012.
797 Fu, F. X., Warner, M. E., Zhang, Y., Feng, Y., and Hutchins, D. A.: Effects of increased
798 temperature and CO_2 on photosynthesis, growth, and elemental ratios in marine
799 *Synechococcus* and *Prochlorococcus* (Cyanobacteria), J. Phycol., 43, 485-496,
800 https://doi.org/10.1111/j.1529-8817.2007.00355.x, 2007.
801 Gao, K., Zhang, Y., and Häder, D.-P.: Individual and interactive effects of ocean
802 acidification, global warming, and UV radiation on phytoplankton, J. Appl.
803 Phycol., 30, 743-759, https://doi.org/10.1007/s10811-017-1329-6, 2018.
804 Gerecht, A. C., Šupraha, L., Edvardsen, B., Probert, I., and Henderiks, J.: High
805 temperature decreases the PIC/POC ratio and increases phosphorus requirements
806 in *Coccolithus pelagicus* (Haptophyta), Biogeosciences, 11, 3531-3545,
807 https://doi.org/10.5194/bg-11-3531-2014, 2014.
808 Gobler, C. J., Doherty, O. M., Hattenrath-Lehmann, T. K., Griffith, A. W., Kang, Y., and
809 Litaker, R. W.: Ocean warming since 1982 has expanded the niche of toxic algal
810 blooms in the North Atlantic and North Pacific oceans, Proceedings of the
811 National Academy of Sciences, 201619575,
812 https://doi.org/10.1073/pnas.1619575114, 2017.
813 Hallegraeff, G. M.: Ocean climate change, phytoplankton community responses, and
814 harmful algal blooms: a formidable predictive challenge, J. Phycol., 46, 220-235,
815 https://doi.org/10.1111/j.1529-8817.2010.00815.x, 2010.
816 Hare, C. E., Leblanc, K., Ditullio, G. R., Kudela, R. M., Zhang, Y., Lee, P. A., Riseman,
817 S., and Hutchins, D. A.: Consequences of increased temperature and CO_2 for

818 phytoplankton community structure in the Bering Sea, Marine Ecology Progress,
819 352, 9-16, https://doi.org/10.3354/meps07182, 2007.
820 Holligan, P., Viollier, M., Harbour, D., Camus, P., and Champagne-Philippe, M.:
821 Satellite and ship studies of coccolithophore production along a continental shelf
822 edge, Nature, 304, 339, https://doi.org/10.1038/304339a0, 1983.
823 Holligan, P. M., Fernández, E., Aiken, J., Balch, W. M., Boyd, P., Burkill, P. H., Finch,
824 M., Groom, S. B., Malin, G., and Muller, K.: A biogeochemical study of the
825 coccolithophore, *Emiliania huxleyi,* in the North Atlantic, Global Biogeochem.
826 Cycles, 7, 879-900, https://doi.org/10.1029/93GB01731, 1993.
827 Hoppe, C., Langer, G., and Rost, B.: *Emiliania huxleyi* shows identical responses to
828 elevated pCO_2 in TA and DIC manipulations, J. Exp. Mar. Bio. Ecol., 406, 54-62,
829 https://doi.org/10.1016/j.jembe.2011.06.008, 2011.
830 Hutchins, D. A., DiTullio, G. R., Zhang, Y., and Bruland, K. W.: An iron limitation
831 mosaic in the California upwelling regime, Limnology & Oceanography, 43, 1037-
832 https://doi.org/1054, 10.4319/lo.1998.43.6.1037, 1998.
833 Hutchins, D. A., and Fu, F.: Microorganisms and ocean global change, Nat Microbiol,
834 2, 17058, https://doi.org/10.1038/nmicrobiol.2017.58, 2017.
835 Iglesias-Rodríguez, M. D., Brown, C. W., Doney, S. C., Kleypas, J., Kolber, D., Kolber,
836 Z., Hayes, P. K., and Falkowski, P. G.: Representing key phytoplankton functional
837 groups in ocean carbon cycle models: Coccolithophorids, Global Biogeochem.
838 Cycles, 16, 47-41-47-20, https://doi.org/10.1029/2001GB001454, 2002.
839 IPCC. Summary for Policymakers. In Climate Change 2013 – The Physical Science

Basis: Working Group I Contribution to the Fifth Assessment Report of the Intergovernmental Panel on Climate Change. Cambridge: Cambridge University Press, 2013

Jiang, L., Sun, Y.-F., Zhang, Y.-Y., Zhou, G.-W., Li, X.-B., McCook, L. J., Lian, J.-S., Lei, X.-M., Liu, S., and Cai, L.: Impact of diurnal temperature fluctuations on larval settlement and growth of the reef coral *Pocillopora damicornis*, Biogeosciences, 14, 5741-5752, https://doi.org/10.5194/bg-14-5741-2017, 2017.

Jiang, H.-B., Fu, F.-X. Rivero-Calle, S., Levine, N., Sañudo-Wilhelmy, S.A., Qu, P.-P., Wang, X.-W., Pinedo Gonzalez, P., Zhu, Z., and Hutchins, D.A., Ocean warming alleviates iron limitation of marine nitrogen fixation. Nature Climate Change, 8, 709–712, doi.org/10.1038/s41558-018-0216-8, 2018.

Keys, M., Tilstone, G., Findlay, H. S., Widdicombe, C. E., and Lawson, T.: Effects of elevated CO_2 and temperature on phytoplankton community biomass, species composition and photosynthesis during an experimentally induced autumn bloom in the western English Channel, Biogeosciences, 15, 3203-3222, https://doi.org/10.5194/bg-15-3203-2018, 2018.

Klaas, C., and Archer, D. E.: Association of sinking organic matter with various types of mineral ballast in the deep sea: Implications for the rain ratio, Global Biogeochem. Cycles, 16, 63-61-63-14, https://doi.org/10.1029/2001GB001765, 2002.

Kling, J.D., Lee, M.D., Fu, F.-X., Phan, M., Wang, X., Qu, P.P., and Hutchins, D.A.: Transient exposure to novel high temperatures reshapes coastal phytoplankton

862 communities. ISME Journal, in press.
863 Kremer, C. T., Fey, S. B., Arellano, A. A., and Vasseur, D. A.: Gradual plasticity alters
864 population dynamics in variable environments: thermal acclimation in the green
865 alga *Chlamydomonas reinhartdii*, Proceedings Biological Sciences, 285,
866 20171942, https://doi.org/10.1098/rspb.2017.1942, 2018.
867 Krumhardt, K. M., Lovenduski, N. S., Iglesias-Rodriguez, M. D., and Kleypas, J. A.:
868 Coccolithophore growth and calcification in a changing ocean, Prog. Oceanogr.,
869 159, 276-295, https://doi.org/10.1016/j.pocean.2017.10.007, 2017.
870 Matson, P. G., Ladd, T. M., Halewood, E. R., Sangodkar, R. P., Chmelka, B. F., and
871 Iglesias-Rodriguez, M. D.: Intraspecific differences in biogeochemical responses
872 to thermal change in the coccolithophore *Emiliania huxleyi*, PLoS One, 11,
873 e0162313, https://doi.org/10.1371/journal.pone.0162313, 2016.
874 Monteiro, F. M., Bach, L. T., Brownlee, C., Bown, P., Rickaby, R. E., Poulton, A. J.,
875 Tyrrell, T., Beaufort, L., Dutkiewicz, S., and Gibbs, S.: Why marine phytoplankton
876 calcify, Science Advances, 2, e1501822, https://doi.org/10.1126/sciadv.1501822,
877 2016.
878 Morán, X. A. G., Lopez-Urrutia, Á., Calvo-Diaz, A., and Li, W. K.: Increasing
879 importance of small phytoplankton in a warmer ocean, Glob. Chang. Biol., 16,
880 1137-1144, https://doi.org/10.1111/j.1365-2486.2009.01960.x, 2010.
881 Neukermans, G., Oziel, L., and Babin, M.: Increased intrusion of warming Atlantic
882 water leads to rapid expansion of temperate phytoplankton in the Arctic, Glob.
883 Chang. Biol., https://doi.org/10.1111/gcb.14075, 2018.

884 Norberg, J.: Biodiversity and ecosystem functioning: a complex adaptive systems
885 approach, Limnol. Oceanogr., 49, 1269-1277,
886 https://doi.org/10.4319/lo.2004.49.4_part_2.1269, 2004.
887 O'Donnell, D. R., Hamman, C. R., Johnson, E. C., Kremer, C. T., Klausmeier, C. A.,
888 and Litchman, E.: Rapid thermal adaptation in a marine diatom reveals constraints
889 and tradeoffs, Glob. Chang. Biol., doi:10.1111/gcb.14360, 2018.
890 Oliver, T., and Palumbi, S.: Do fluctuating temperature environments elevate coral
891 thermal tolerance?, Coral Reefs, 30, 429-440, https://doi.org/10.1007/s00338-011-
892 0721-y, 2011.
893 Paasche, E.: Reduced coccolith calcite production under light-limited growth: a
894 comparative study of three clones of *Emiliania huxleyi* (Prymnesiophyceae),
895 Phycologia, 38, 508-516, 1999.
896 Paasche, E.: A review of the coccolithophorid *Emiliania huxleyi* (Prymnesiophyceae),
897 with particular reference to growth, coccolith formation, and calcification-
898 photosynthesis interactions, Phycologia, 40, 503-529,
899 https://doi.org/10.2216/i0031-8884-40-6-503.1, 2001.
900 Platt, T., Gallegos, C. L., & Harrison, W. G.: Photoinhibition of photosynthesis in
901 natural assemblages of marine-phytoplankton. Journal of Marine Research, 38(4),
902 687-701, 1980.
903 Qu, P., Fu, F., and Hutchins, D. A.: Responses of the large centric diatom *Coscinodiscus*
904 sp. to interactions between warming, elevated CO_2, and nitrate availability,
905 Limnology & Oceanography, 63, https://doi.org/10.1002/lno.10781, 2018.

Qu, P., Fu, F.-X., Kling, J. D., Huh, M., Wang, X., and Hutchins, D. A.: Distinct responses of the nitrogen-fixing marine cyanobacterium *Trichodesmium* to a thermally variable environment as a function of phosphorus availability, Frontiers in Microbiology, 10, https://doi.org/10.3389/fmicb.2019.01282, 2019.

Rasconi, S., Winter, K., and Kainz, M. J.: Temperature increase and fluctuation induce phytoplankton biodiversity loss–Evidence from a multi-seasonal mesocosm experiment, Ecology and Evolution, 7, 2936-2946, https://doi.org/10.1002/ece3.2889, 2017.

Raven, J. A., and Crawfurd, K.: Environmental controls on coccolithophore calcification, Mar. Ecol. Prog. Ser., 470, 137-166, https://doi.org/10.3354/meps09993, 2012.

Riegman, R., Stolte, W., Noordeloos, A. A., and Slezak, D.: Nutrient uptake and alkaline phosphatase (EC 3: 1: 3: 1) activity of *Emiliania huxleyi* (Prymnesiophyceae) during growth under N and P limitation in continuous cultures, J. Phycol., 36, 87-96, https://doi.org/10.1046/j.1529-8817.2000.99023.x, 2000.

Rosas-Navarro, A., Langer, G., and Ziveri, P.: Temperature affects the morphology and calcification of *Emiliania huxleyi* strains, Biogeosciences, 13, 2913-2926, https://doi.org/10.5194/bg-13-2913-2016, 2016.

Safaie, A., Silbiger, N. J., McClanahan, T. R., Pawlak, G., Barshis, D. J., Hench, J. L., Rogers, J. S., Williams, G. J., and Davis, K. A.: High frequency temperature variability reduces the risk of coral bleaching, Nat Commun, 9,

https://doi.org/10.1038/s41467-018-04074-2, 2018.

Schaum, C. E., and Collins, S.: Plasticity predicts evolution in a marine alga, Proceedings of the Royal Society B: Biological Sciences, 281, 20141486, https://doi.org/10.1098/rspb.2014.1486, 2014.

Schaum, C. E., Buckling, A., Smirnoff, N., Studholme, D., and Yvon-Durocher, G.: Environmental fluctuations accelerate molecular evolution of thermal tolerance in a marine diatom, Nat Commun, 9, 1719, https://doi.org/10.1038/s41467-018-03906-5, 2018.

Schaum, E., Rost, B., Millar, A. J., and Collins, S.: Variation in plastic responses of a globally distributed picoplankton species to ocean acidification, Nature Climate Change, 3, 298-302, https://doi.org/10.1038/NCLIMATE1774, 2013.

Schlüter, L., Kai, T. L., Gutowska, M. A., Gröger, J. P., Riebesell, U., and Reusch, T. B. H.: Adaptation of a globally important coccolithophore to ocean warming and acidification, Nature Climate Change, 4, 1024-1030, https://doi.org/10.1038/nclimate2379, 2014.

Sett, S., Bach, L. T., Schulz, K. G., Koch-Klavsen, S., Lebrato, M., and Riebesell, U.: Temperature modulates coccolithophorid sensitivity of growth, photosynthesis and calcification to increasing seawater pCO_2, PLoS One, 9, e88308, https://doi.org/10.1371/journal.pone.0088308, 2014.

Shurin, J. B., Winder, M., Adrian, R., Keller, W., Matthews, B., Paterson, A. M., Paterson, M. J., Pinel-Alloul, B., Rusak, J. A., and Yan, N. D.: Environmental stability and lake zooplankton diversity–contrasting effects of chemical and

thermal variability, Ecol. Lett., 13, 453-463, https://doi.org/10.1111/j.1461-0248.2009.01438.x, 2010.

Solórzano, L., and Sharp, J. H.: Determination of total dissolved phosphorus and particulate phosphorus in natural waters, Limnology & Oceanography, 25, 754-758, https://doi.org/10.4319/lo.1980.25.4.0754, 1980.

Sunda, W. G., Price, N. M., and Morel, F. M.: Trace metal ion buffers and their use in culture studies, Algal Culturing Techniques, 4, 35-63, 2005.

Sunday, J. M., Bates, A. E., and Dulvy, N. K.: Thermal tolerance and the global redistribution of animals, Nature Climate Change, 2, 686, https://doi.org/10.1038/nclimate1539, 2012.

Tatters, A. O., Schnetzer, A., Xu, K., Walworth, N. G., Fu, F., Spackeen, J. L., Sipler, R. E., Bertrand, E. M., McQuaid, J. B., Allen, A. E, Bronk, D.A., Gao, K., Sun, J., Caron, D.A., and Hutchins, D.A.: Interactive effects of temperature, CO_2 and nitrogen source on a coastal California diatom assemblage, J. Plankton Res., 40, 151-164, 2018.

Thomas, M. K., Kremer, C. T., Klausmeier, C. A., and Litchman, E.: A global pattern of thermal adaptation in marine phytoplankton, Science, 338, 1085-1088, https://doi.org/10.1126/science.1224836, 2012.

Vázquez, D. P., Gianoli, E., Morris, W. F., and Bozinovic, F.: Ecological and evolutionary impacts of changing climatic variability, Biological Reviews, 92, 22-42, https://doi.org/10.1111/brv.12216, 2017.

Vasseur, D. A., DeLong, J. P., Gilbert, B., Greig, H. S., Harley, C. D., McCann, K. S.,

Savage, V., Tunney, T. D., and O'Connor, M. I.: Increased temperature variation poses a greater risk to species than climate warming, Proceedings of the Royal Society of London B: Biological Sciences, 281, 20132612, https://doi.org/10.1098/rspb.2013.2612, 2014.

Westbroek, P., Brown, C. W., van Bleijswijk, J., Brownlee, C., Brummer, G. J., Conte, M., Egge, J., Fernández, E., Jordan, R., and Knappertsbusch, M.: A model system approach to biological climate forcing. The example of *Emiliania huxleyi*, Global Planet. Change, 8, 27-46, 1993.

Yvon-Durocher, G., Allen, A. P., Cellamare, M., Dossena, M., Gaston, K. J., Leitao, M., Montoya, J. M., Reuman, D. C., Woodward, G., and Trimmer, M.: Five years of experimental warming increases the biodiversity and productivity of phytoplankton, PLoS Biol., 13, e1002324, https://doi.org/10.1371/journal.pbio.10023242015.

Zander, A., Bersier, L. F., and Gray, S. M.: Effects of temperature variability on community structure in a natural microbial food web, Glob. Chang. Biol., 23, 56-67, https://doi.org/10.1111/gcb.13374, 2017.

Zhang, M., Qin, B., Yu, Y., Yang, Z., Shi, X., and Kong, F.: Effects of temperature fluctuation on the development of cyanobacterial dominance in spring: Implication of future climate change, Hydrobiologia, 763, 135-146, https://doi.org/10.1007/s10750-015-2368-0, 2016.

Zhang, Y., Klapper, R., Lohbeck, K. T., Bach, L. T., Schulz, K. G., Reusch, T. B. H., and Riebesell, U.: Between- and within-population variations in thermal reaction

norms of the coccolithophore *Emiliania huxleyi*, Limnol. Oceanogr., 59, 1570-1580, https://doi.org/10.4319/lo.2014.59.5.1570, 2014.

Zhu, Z., Qu, P., Fu, F., Tennenbaum, N., Tatters, A. O., and Hutchins, D. A.: Understanding the blob bloom: Warming increases toxicity and abundance of the harmful bloom diatom *Pseudo-nitzschia* in California coastal waters, Harmful Algae, 67, 36-43, https://doi.org/10.1016/j.hal.2017.06.004, 2017.

Figure legends:

Fig. 1 Thermal performance curve showing cell-specific growth rates (d^{-1}) of *Emiliania huxleyi* CCMP371 across a temperature range from 8.5 to 28.6 ℃. Symbols represent means and error bars are the standard deviations of three replicates at each temperature, but in many cases the errors bars are smaller than the symbols.

Fig. 2 Changes in *Emiliania huxleyi* TPC/PON ratios (**A**), POC/PON ratios (**B**), PIC/POC ratios (**C**) and Cha/POC ratios (**D**) across a temperature range from 8.5 to 28.6 ℃. Dashed lines represent the average ratios for the entire temperature range. Bars represent means and error bars are the standard deviations of three replicates at each temperature. Symbols * represent the significant difference ($p<0.05$) between average ratios and the ratio at each temperature.

Fig. 3 *Emiliania huxleyi* growth rate responses to constant temperatures, and during the warm and cool phases of the two thermal variation frequencies (one-day and two-day), under low (**A**) and high (**B**) mean temperatures. The thick black line in the boxplots represent median values for each experimental treatment; whiskers on boxplots indicate 1.5 × interquartile range. Listed p-values with their respective brackets are the statistical significance between two treatments.

Fig. 4 Responses of *Emiliania huxleyi* PIC/POC ratios to constant temperatures, and during the warm and cool phases of two thermal variation frequencies (one-day and two-day), under low (**A**) and high (**B**) mean temperatures. LT: Low temperature; HT: High temperature. The thick black line in the boxplots represent median values for each experimental treatment; whiskers on boxplots indicate 1.5 × interquartile range. Listed

1023 p-values with their respective brackets denote the statistical significance between two
1024 treatments.

1025 **Fig. 5** Responses of *Emiliania huxleyi* photosynthetic carbon fixation and calcification
1026 at constant temperatures and during the warm and cool phases of two thermal variation
1027 frequencies (one-day and two-day), including: total carbon fixation (photosynthesis +
1028 calcification) at low (**A**) and high (**B**) temperatures; photosynthetic carbon fixation at
1029 low (**C**) and high (**D**) temperatures; and calcification rates at low (**E**) and high (**F**)
1030 temperatures. LT: Low temperature; HT: High temperature. The thick black line in
1031 the boxplots represent median values for each experimental treatment; whiskers on
1032 boxplots indicate 1.5 × interquartile range. Listed p-values with their respective
1033 brackets denote the statistical significance between two treatments.

1034 **Fig. 6** Responses of *Emiliania huxleyi* calcification to photosynthesis ratios (cal/photo)
1035 to constant temperatures, and during the warm and cool phases of two thermal variation
1036 frequencies (1 day and 2 day), under low (**A**) and high (**B**) mean temperatures. LT: Low
1037 temperature; HT: High temperature. The thick black line in the boxplots represent
1038 median values for each experimental treatment; whiskers on boxplots indicate 1.5 ×
1039 interquartile range. Listed p-values with their respective brackets denote the statistical
1040 significance between two treatments.

1041 **Fig. 7** Responses of *Emiliania huxleyi* elemental ratios in two thermal variation
1042 frequency treatments (1 day and 2 day) compared to constant temperatures, for:
1043 TPC/PON (**A**, cool phase and **B**, warm phase), PON/POP (**C**, cool phase and **D**, warm
1044 phase) and Chl *a*/POC ratios (**E**, cool phase and **F**, warm phase). LT: Low temperature;

1045 HT: High temperature. The thick black line in the boxplots represent median values for
1046 each experimental treatment; whiskers on boxplots indicate 1.5 × interquartile range.
1047 Listed p-values with their respective brackets denote the statistical significance between
1048 two treatments.

1049 **Fig. 8** Thermal performance curves based on specific growth rates (d^{-1}) of *Emiliania*
1050 *huxleyi*, including our experimentally determined constant condition temperature
1051 performance curve (black symbols and solid line) and a predicted fluctuating condition
1052 temperature performance curve (dashed line) according to the model of Bernhardt et al.
1053 (2018). Measured growth rates from the two low and high temperature experiments
1054 are shown for constant thermal conditions (red symbols), one-day (green symbols) and
1055 two-day (blue symbols) variation treatments.

1056

Table 1 The effect of temperature variation under low and high temperature on total carbon (pg/cell), cellular POC (pg/cell), cellular PIC (pg/cell), cellular PON (pg/cell), cellular POP (pg/cell) and cellular Chl *a* (pg/cell) of *Emiliania huxleyi.*

Treatment		Total Carbon	Cellular PON	Cellular POP	Cellular POC	Cellular PIC	Cellar Chl *a*
Low temperature	18.5 °C	11.5±0.4	1.8±0.2	0.17±0.00	8.0±0.6	3.5±0.3	0.14±0.00
	One-day cool point (16)	13.0±0.5	2.2±0.3	0.18±0.00	8.9±0.3	4.1±0.3	0.15±0.01
	One-day warm point (21)	12.0±0.7	2.1±0.3	0.19±0.00	9.3±0.9	2.7±0.9	0.19±0.00
	Two-day cool point (16)	10.1±0.7	1.3±0.2	0.16±0.01	6.0±0.9	4.0±0.3	0.12±0.01
	Two-day warm point (21)	10.4±0.5	1.5±0.2	0.17±0.01	6.6±0.5	3.8±0.3	0.15±0.01
High temperature	25.5 °C	15.0±0.7	2.0±0.1	0.21±0.01	9.5±0.3	5.5±0.7	0.18±0.02
	One-day cool point (23)	16.1±1.4	3.0±0.2	0.21±0.00	12.9±1.5	3.2±0.2	0.15±0.01
	One-day warm point (28)	19.1±0.8	4.4±0.3	0.24±0.01	17.0±0.6	2.1±0.2	0.20±0.02
	Two-day cool point (23)	12.4±1.0	1.9±0.2	0.19±0.01	7.5±1.0	4.8±0.3	0.13±0.01
	Two-day warm point (28)	19.4±2.0	3.9±0.8	0.25±0.03	18.3±3.7	2.1±0.9	0.25±0.02

1061 **Fig. 1**

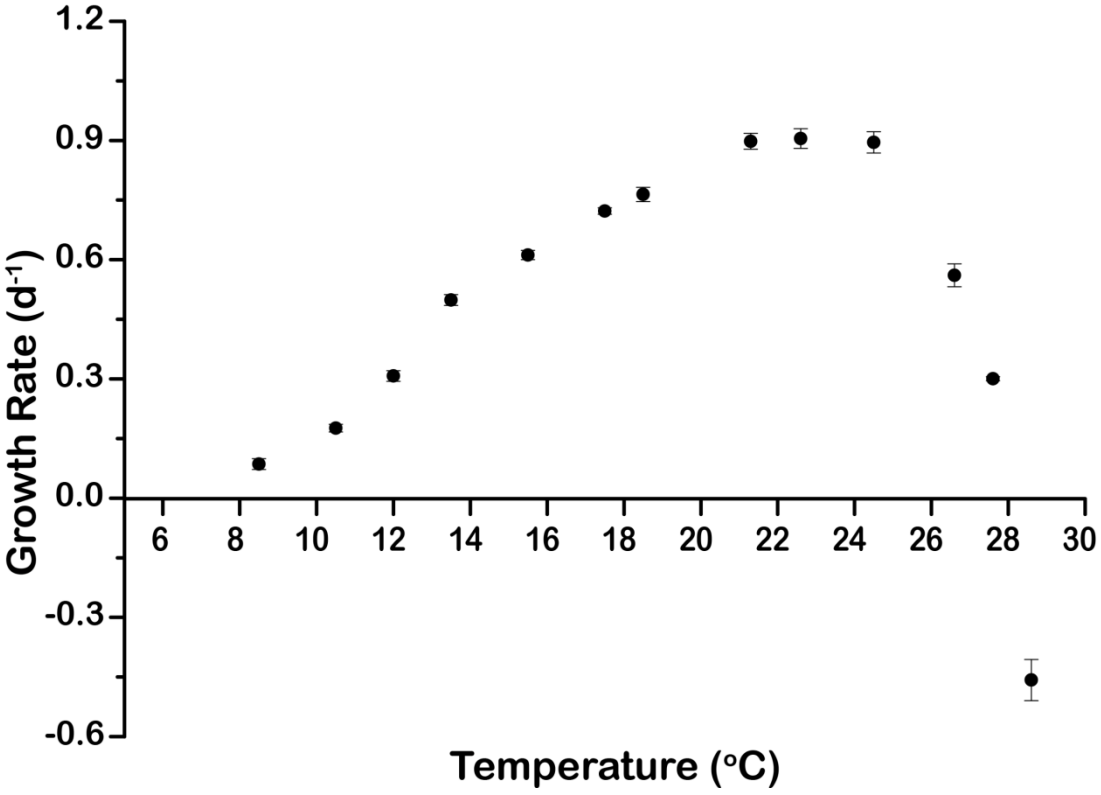

1062

1063 **Fig. 2**

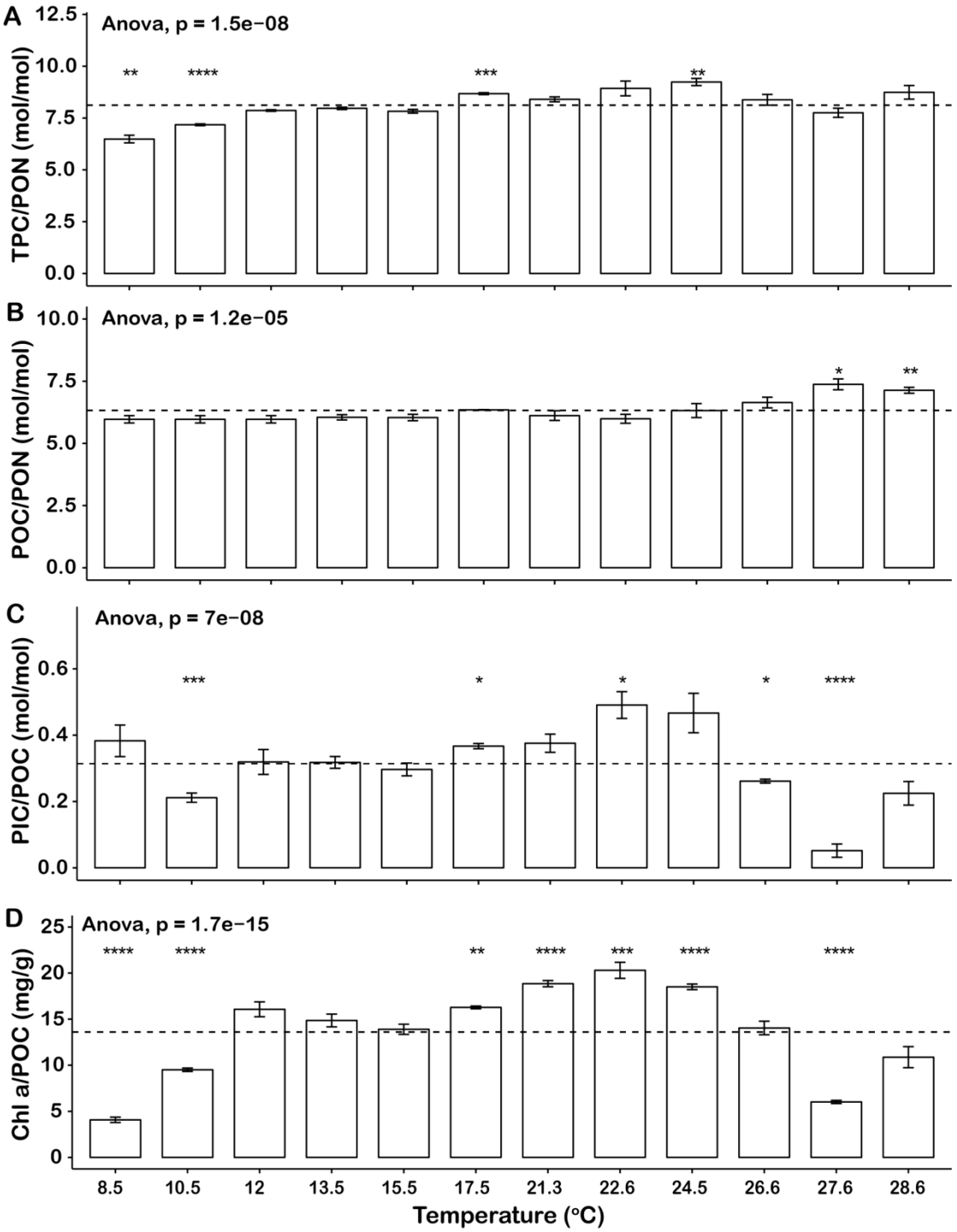

1064

1065

1066 **Fig. 3**

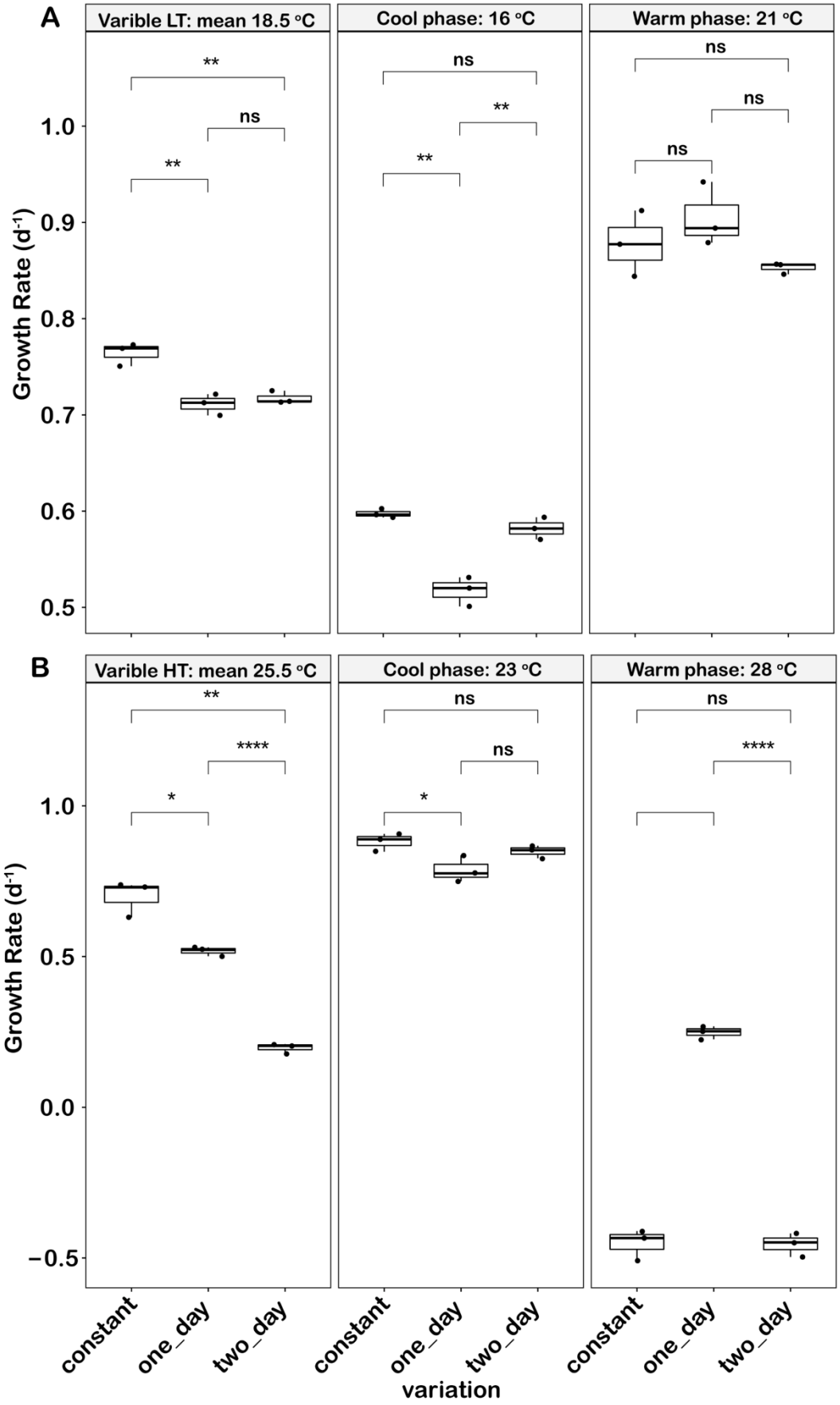

1067

1068 **Fig. 4**

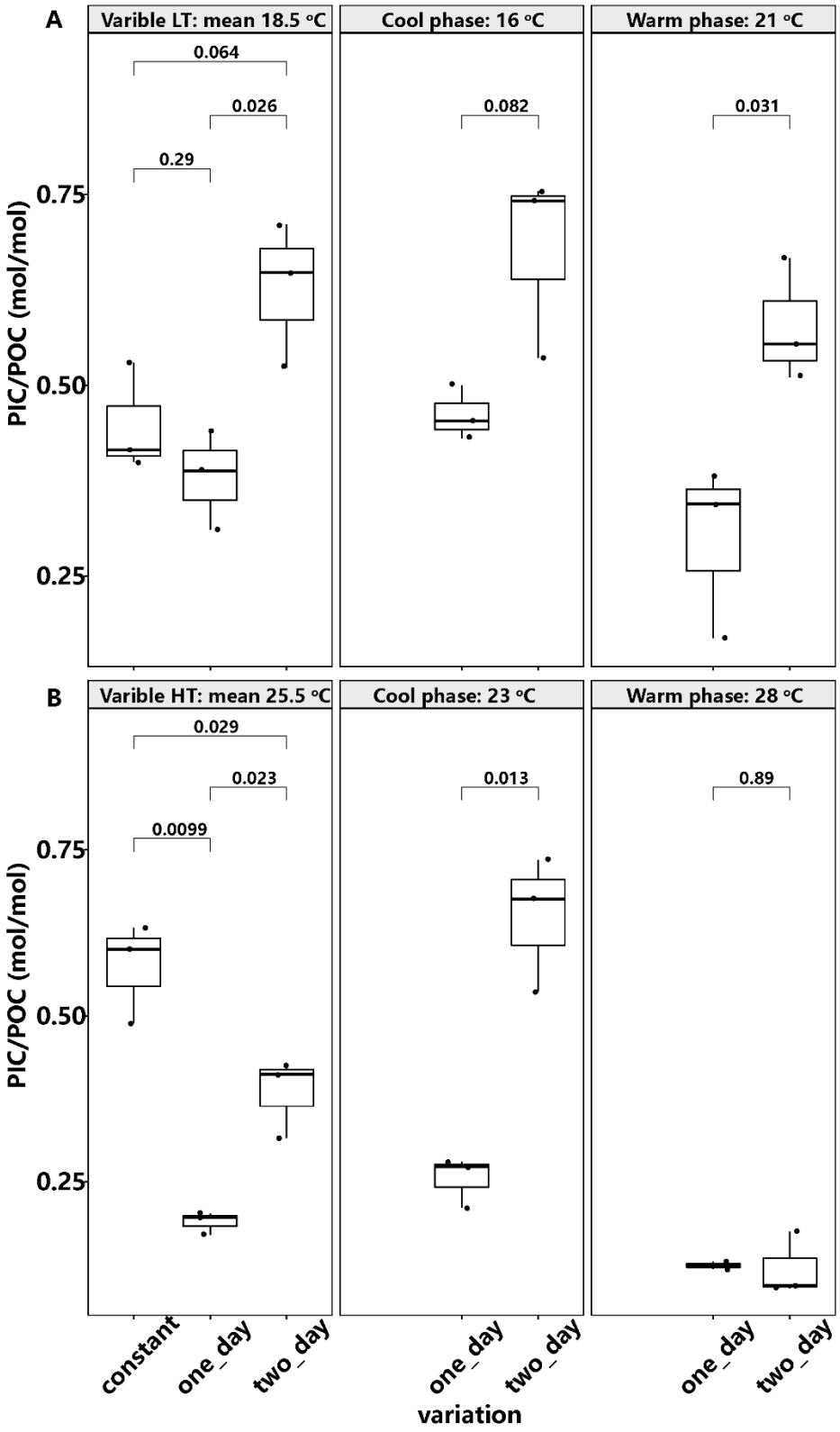

1069

1070

Fig. 5

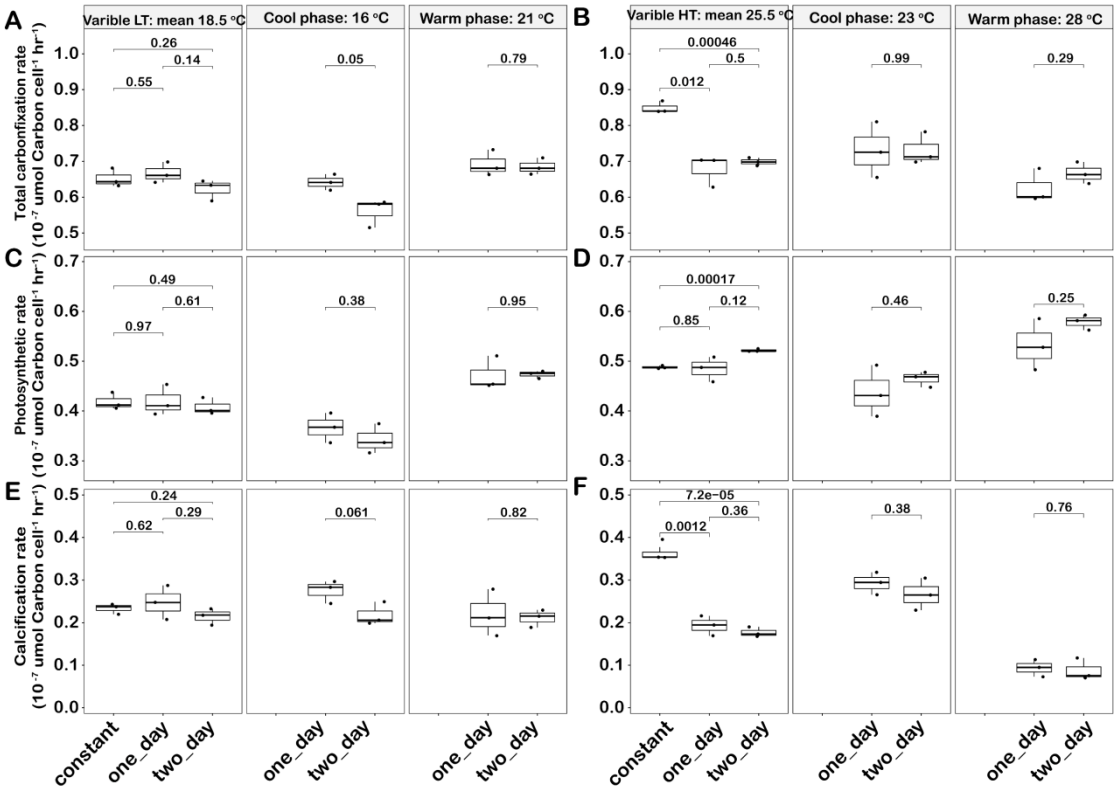
A
Varible LT: mean 18.5 °C
Cool phase: 16 °C
Warm phase: 21 °C
B
Varible HT: mean 25.5 °C
Cool phase: 23 °C
Warm phase: 28 °C
Total carbonfixation rate (10⁻⁷ umol Carbon cell⁻¹ hr⁻¹)
C
D
Photosynthetic rate (10⁻⁷ umol Carbon cell⁻¹ hr⁻¹)
E
F
Calcification rate (10⁻⁷ umol Carbon cell⁻¹ hr⁻¹)
0.26
0.14
0.55
0.05
0.79
0.00046
0.5
0.012
0.99
0.29
0.49
0.61
0.97
0.38
0.95
0.00017
0.12
0.85
0.46
0.25
0.24
0.29
0.62
0.061
0.82
7.2e−05
0.36
0.0012
0.38
0.76
constant
one_day
two_day

Fig. 6

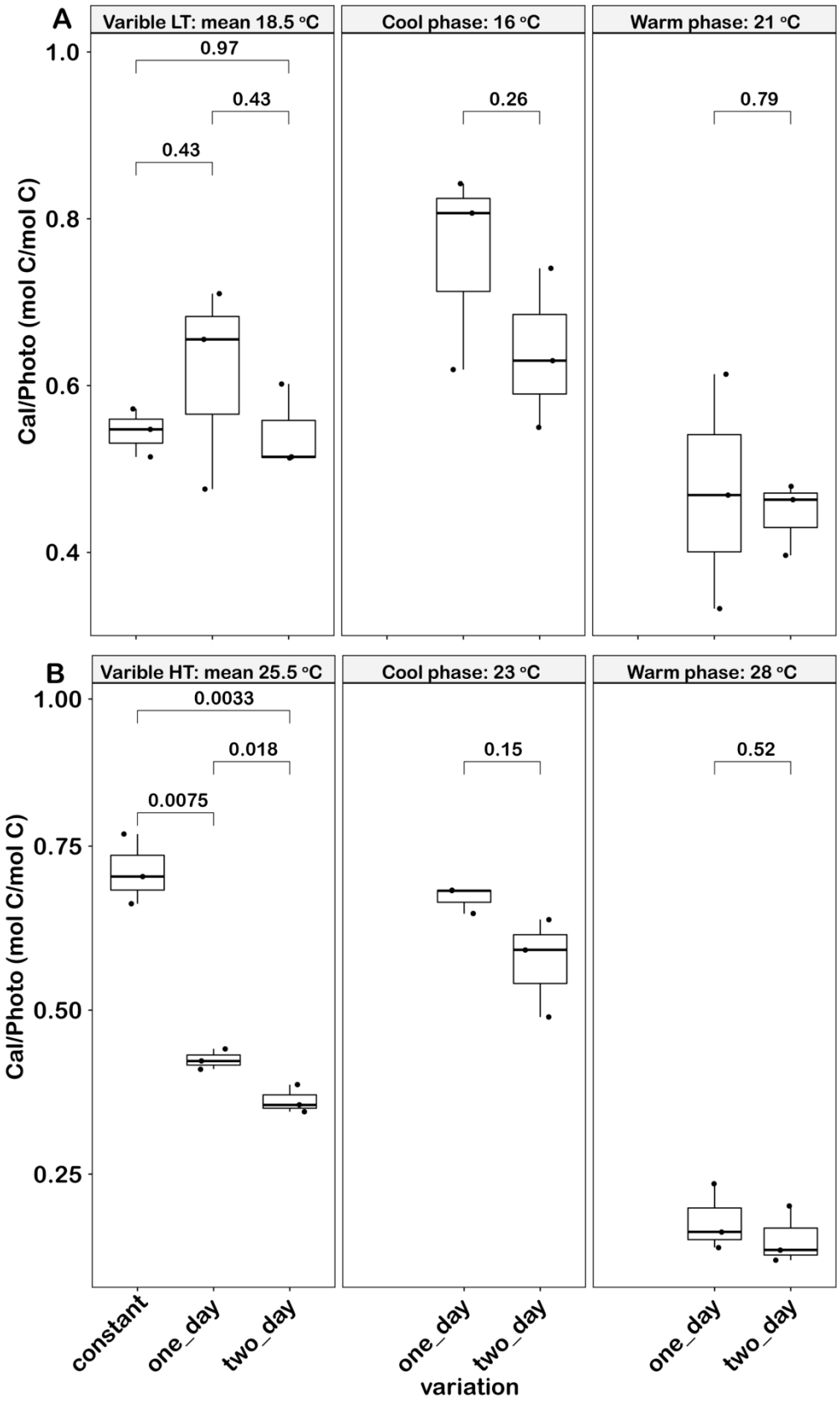
A
Varible LT: mean 18.5 °C
Cool phase: 16 °C
Warm phase: 21 °C
0.97
0.43
0.43
0.26
0.79
Cal/Photo (mol C/mol C)
1.0
0.8
0.6
0.4
B
Varible HT: mean 25.5 °C
Cool phase: 23 °C
Warm phase: 28 °C
0.0033
0.018
0.0075
0.15
0.52
Cal/Photo (mol C/mol C)
1.00
0.75
0.50
0.25
constant
one_day
two_day
one_day
two_day
one_day
two_day
variation

Fig. 7

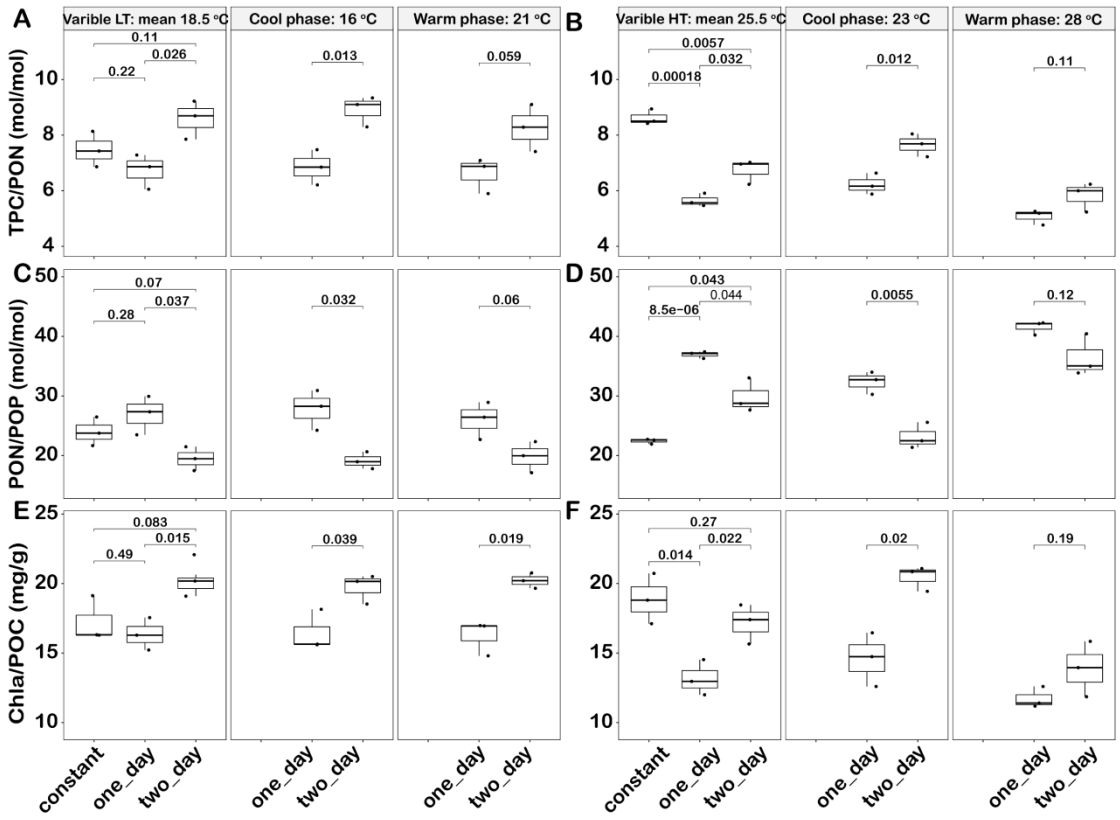
A
Varible LT: mean 18.5 °C
Cool phase: 16 °C
Warm phase: 21 °C
B
Varible HT: mean 25.5 °C
Cool phase: 23 °C
Warm phase: 28 °C
TPC/PON (mol/mol)
PON/POP (mol/mol)
Chla/POC (mg/g)
C
D
E
F
0.11
0.22
0.026
0.013
0.059
0.0057
0.00018
0.032
0.012
0.11
0.07
0.28
0.037
0.032
0.06
0.043
8.5e−06
0.044
0.0055
0.12
0.083
0.49
0.015
0.039
0.019
0.27
0.014
0.022
0.02
0.19
constant
one_day
two_day

1081 **Fig. 8**

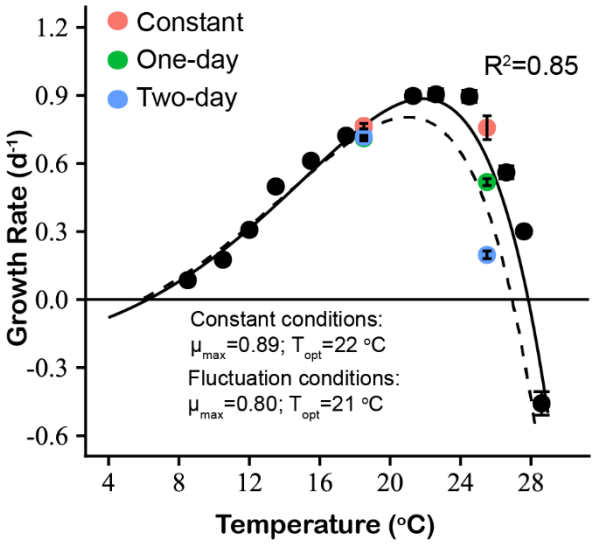

1082